2004

Molecular Typing Of Mycobacterial Isolates Cultured From The Tissue Of Inflammatory Bowel Disease (Crohn's Disease) Patients

Leanne M. Adams
University of Central Florida

MOLECULAR TYPING OF MYCOBACTERIAL ISOLATES CULTURED FROM THE TISSUE OF INFLAMMATORY BOWEL DISEASE (CROHN'S DISEASE) PATIENTS

by

LEANNE ADAMS
B.S. GROVE CITY COLLEGE, 1996

A thesis submitted in partial fulfillment of the requirements
for the degree of Master of Science
in the Department of Molecular Biology and Microbiology
in the College of Health and Public Affairs
at the University of Central Florida
Orlando, Florida

Spring Term

2004

ABSTRACT

The role of *Mycobacterium avium* subsp *paratuberculosis* (MAP) in the etiology and pathogenesis of inflammatory bowel disease (IBD) including Crohn's Disease (CD), has been investigated. The fastidious characteristics and cross reactivity of MAP with other members in *Mycobacteria* have produced significant challenges in their detection and identification. In this two year pilot study, an array of three PCR molecular assays based on the detection of sequences from the16S rRNA, IS1245, and IS900 genes, belonging to members of the MAC, have been developed and optimized into a common protocol to be used as a rapid and accurate diagnostic tool regarding *M. avium complex* (MAC) infection. The PCR protocol time was reduced by half, and the sensitivity and specificity of the molecular assays has been significantly improved barring the need for southern hybridization. This improved methodology was employed for the molecular typing of MAC in 100 resected, full-thickness tissue samples removed from IBD patients. The tissue samples were homogenized, decontaminated, and inoculated into two mycobacterial culture media systems. A total of 328 Bactec and Mycobacteria Growth Indicator Tube (MIGT) cultures were evaluated for positive MAC growth. Harvested cells were then subjected to genomic DNA extraction and subsequent PCR typing. The I6 S rRNA-based PCR resulted in detection of 26/28 (93%) MAC in Bactec cultures. Specifically, 25/28 (89%) of positive MAC indicated the presence of IS1245 specific to *M. avium* subsp *avium* (MAV), and 6/28 (21%) produced results consistent with the presence of IS900 following nested PCR. Moreover, 20/100 (20%) of MGIT cultures were positive for MAP. Sequence analysis was performed on amplified regions of the IS900 element from seven isolates. A nucleotide alignment revealed that 2/7 isolates demonstrated 100% homology to Bovine MAP and 5/7

isolates showed 96-99% homology to sequenced Bovine MAP published in GenBank. The detection of at least two Bovine derived MAP in IBD tissue will have great impact on the epidemiology and reclassification of IBD. The significant homology of the other five isolates to Bovine derived MAP suggests a diversity in the geographical distribution of MAP regarding Johne's disease and CD. Ultimately, the etiology, diagnosis, and the treatment of IBD as well as control and prevention measures may be enhanced with better tools for investigating emerging infectious diseases.

.

I would like to dedicate this manuscript to Mr. David Browdy and the thousands of people like him who suffer with Crohn's disease everyday. It is my hope that someday, through more research, we will conquer this devastating disease. I would also like to dedicate this work to my grandparents, Howard and Margaret Gross, whose continued love, encouragement, and interest supported me throughout my academic career.

ACKNOWLEDGMENTS

I would like to thank the Department of Molecular Biology and Microbiology at the University of Central Florida for allowing me the opportunity and support to further my education. Dr. Henry Daniell and Dr. Roseann White, my committee members, gave me the use of their facilities as well as helpful information through their classes and conversation. I would like to acknowledge Dr. Sreevastan at Ohio State University for collaborating on this project. Also, I would like to thank all the patients who participated in this study. This research could have never been possible without them. In addition, I would like to thank Claudia Romero for her technical advice and support regarding this project and Shin-chieh (Bonnie) Yang for her support and encouragement during classes and in the laboratory. I would also like to thank Dr. George Ghobrial for his friendship and the skills he taught me. I will miss our interesting conversations as well as his wife's delicious cookies. I would like to thank Cynthia Cardona for her friendship and many thoughtful prayers and words of encouragement. It really helped to share my experiences with someone who was also working on her thesis. I would particularly like to thank Barbara Knowles, my mother, for her writing expertise and emotional support. Her faith in me has always given me the strength to reach farther than I ever thought I could. I would like to thank Bill Adams, my husband, for his unending love, encouragement, and support. I truly could not have completed this project without him. I would also like to thank William Adams, my new son, for making everyday a good day and inspiring me to complete this work that I may be a better role model for him. And finally, I would like to thank Dr. Saleh Naser for his commitment and dedication to Crohn's disease research and its patients. His leadership, guidance, patience, and support has helped me realize my academic goals.

TABLE OF CONTENTS

LIST OF FIGURES.....ix

LIST OF TABLES.....xi

LIST OF ABBREVIATIONS.....xii

INTRODUCTION.....1

History of Crohn’s Disease.....1

Clinical Aspect of Crohn's Disease.....2

Crohn’s Disease Epidemiology: Incidence and Prevalence.....3

Crohn’s Disease Diagnosis and Methodology.....4

Crohn’s Disease and Mycobacteria.....5

Crohn’s Disease Etiology: Theories and Reality.....6

The Genetic Susceptibility Factor.....7

Why is Mycobacterium a Good Candidate for Crohn's Disease Pathogenesis?.....8

The Host Immune Response.....11

Spheroplast Versus Bacillary.....13

Variability in Laboratory Techniques.....14

Rationale and Objectives 15

MATERIALS AND METHODS.....17

Specimen Processing.....17

Specimen Collection and Logging.....17

Homogenization and Decontamination.....17

.....20

Culture and Growth Condition.....21
The Bactec Culture System.....21
Bactec 460 TB Growth Detector.....22
The MGIT (Mycobacterial Growth Indicator Tube) culture system.....23
Subculture Media.....26
Genomic DNA Extraction.....26
PCR Analysis.....27
The Oligonucleotide Primers.....27
Optimization of the PCR Condition 28
PCR Controls.....29
Agarose Gel Electrophoresis Analysis.....29
Microscopic Analysis 30
DNA Purification.....31
DNA Quantification.....32
DNA Sequencing and Analysis.....33
RESULTS.....37
Optimization.....37
Specimen Processing.....55
Mycobacterial Growth in Bactec Media.....60
Subculture of Mycobacteria Grown in Bactec Media.....76
Mycobacterial Growth in MGIT Media.....82
Sequence Analysis of Amplified IS900 DNA Fragments.....87
DISCUSSION.....92

CONCLUSION.....95

LIST OF REFERENCES.....96

LIST OF FIGURES

Figure 1. Documentation and Tracking Form for each Tissue Received.....19

Figure 2. Photograph and Schematic Diagram of the Bactec 460 TB Analyzer.....24

Figure 3. Illustration of Amplified Regions of the IS900 Gene following Nested PCR using Primer Sets P90/P91 and Av1/Av2.....35

Figure 4. Early PCR Optimization Results using Av22a/Av22b oligonucleotide primers for the detection of MAC.....39

Figure 5. Optimization of MgCl2 versus Oligonucleotide Primer Concentrations in Hspx PCR Assay.....41

Figure 6. PCR Optimization of Different DNA Taq Polymerases versus Thermocycling Conditions in the Detection of MAP using P90/P91 primer set.....45

Figure 7-I. Thermocycler Protocols and PCR Reagent Concentrations after Optimization.....49

Figure 7-II. Thermocycler Protocols and PCR Reagent Concentrations before Optimization.…51

Figure 8. Comparison of Early Optimization Trials versus Final Optimization Trials for all PCR Assays used in this Study.....53

Figure 9. 16 S rRNA PCR Assay Results for Representative Set of Bactec Cultures. 64

Figure 10. IS1245 PCR Assay Results for Representative Set of Bactec Cultures.....67

Figure 11. IS900 Nested PCR Assay Results for Representative Set of Bactec Cultures.....71

Figure 12. Comparison of MAC Atypical versus Typical Acid-fast Bacilli Obtained from Bactec Subcultures.....77

Figure 13. Complete PCR Results for a Representative Set of Bactec Subcultures.....79

Figure 14. 16 S rRNA PCR Assay Results on a Representative Set of MGIT Cultures.....83

Figure 15. IS900 Nested PCR Assay Results for a Representative Set of MGIT Cultures.....85

Figure 16. Alignment of IS900 Blast Results following Nucleotide Sequencing.....90

LIST OF TABLES

Table 1: Primer Selections for PCR Panel to Detect and Distinguish Members of MAC.....44

Table 2: Tissue Processing and Growth Time in Bactec Media.....56

Table 3: Documentation of Received IBD Tissues and Media Types Used for Samples 1-37….58

Table 4: Documentation of Received IBD Tissues and Media Types Used for Samples 38-74…59

Table 5: Documentation of Received IBD Tissues and Media Types Used for Samples 75-100. 60

Table 6: Acid-fast Results on Bactec Cultures and Subcultures.....62

Table 7: Results of the 16S rRNA PCR Assay on Positive Bactec Cultures.....63

Table 8: Results of the IS1245 PCR Assay on Positive Bactec Cultures.....69

Table 9: Results of the IS900 Nested PCR Assay on Positive Bactec Cultures.....70

Table 10: Summary of Three Assays on Bactec Cultures.....74

Table 11: IS900 DNA Copy Number in Samples that Tested IS900 Positive after Nested PCR..75

Table 12: Results of the 16S rRNA, IS1245, and IS900 nested PCR Assays on Positive Bactec Subcultures.....81

Table 13: Pairwise Comparison Matrix of IS900 Nucleotide Sequences.....89

LIST OF ABBREVIATIONS

B-E – Bactec minus egg yolk

B+E – Bactec plus egg yolk

CD – Crohn's disease

DMSO – Dimethyl sulfoxide

GI – Gastrointestinal

GPL – Glycopeptidolipid

HIV – Human Immunodeficiency virus

IBD – Inflammatory Bowel disease

IL-12 – Interleukin-12

INF-gamma – Interferon gamma

IS1245 – Insertional sequence 1245

IS900 – Insertional sequence 900

JD – Johne's Disease

MAC – Mycobacterium avium complex

MAP – Mycobacterium avium subspecies paratuberculosis

MAS – Mycobacterium avium silvaticum

MAV – Mycobacterium avium subspecies avium

MDP – muramyl dipeptide

MGIT – Mycobacterial growth indicator tube

MI – Mycobacterium intercellulare

NBS-LRR – Nucleotide-binding site-leucine rich repeat

NOD2/CARD15 – Nucleotide-binding oligomerization domain 2/ Capsase-activating recruitment domain 15

OADC – Oleic acid, bovine albumin, dextrose, catalase

PBS – Phosphate buffer solution

PCR – Polymerase chain reaction

TE – Tris EDTA

TH-1 – T helper cell 1

TH-2 – T helper cell 2

TNF-alpha – Tumor necrosis factor alpha

UC – Ulcerative colitis

INTRODUCTION

History of Crohn's Disease

In 1932, B.B. Crohn, along with colleagues Ginzberg and Oppenheimer, published a landmark paper entitled "Regional Ileitis" that would forever coin a disease while sparking deep controversy in the scientific community that still lingers today (14, 10). Although the term Crohn's disease (CD) is a relatively new term, the disease itself is thought to have first been described in 1682 (36, 10). It was Dalziel, however, in 1913, that laid the groundwork for the recognition of CD as distinct from other intestinal disorders, when he observed striking similarities between what he termed "intestinal enteritis" and pseudotuberculosis found in cattle (17), today called paratuberculosis or Johne's disease (JD) (10, 73). Often confused with intestinal tuberculosis, this chronic enteritis so mirrored Johne's both pathologically and histologically that logical suspicions arose that they may share the same acid-fast bacilli as their etiological agent (13, 10). Although Dalziel was unsuccessful in isolating mycobacteria from the intestinal enteritis patients, he still held fast to an infectious etiological theory stating (17, 10): "In many cases the absence of acid-fast bacilli would suggest a clear distinction, but the histological characters are so similar as to justify a proposition that the diseases may be the same." But, without clear evidence for a bacterial origin, the mycobacterial theory for this baffling disease faded in the scientific community (52, 10). Thus, the intestinal disorder was reclassified as a tubercle disease until Crohn distinguished it once again as a separate ailment.

However, because he was unable to fulfill Koch's postulates, he proposed CD as an autoimmune disorder (14, 10). And thus, to this day, the scientific community continues to grapple with the origins of this disease, with new technologies sparking renewed interest into the old theory that CD will some day be demonstrated to have a mycobacterial etiology.

Clinical Aspect of Crohn's Disease

Crohn's is a type of inflammatory bowel disease usually manifesting itself in the terminal ileum. However, any part of the gastrointestinal (GI) tract can be involved including the mouth, larynx, esophagus, stomach, and colon. Crohn's cases have also been demonstrated in the muscle, synovial tissue, bone, and skin (10). This chronic enteritis differs from other colitis diseases in that it causes transmural inflammation of the gut characterized by non-caseating granulomas, micro-fistula formation, and ulcerative fissures (57, 50). These deep clefts cause the intestinal mucosa to become patchy and segmented and give the appearance of cobblestone, a classic symptom of Crohn's (22). Other common features include pain and tenderness in the lower right quadrant mimicking acute appendicitis. Intestinal stenosis also occurs causing obstruction of the lumen, abdominal distention, constipation, and occasionally vomiting. Intestinal bleeding due to granulomatous and ulcerative lesions can induce diarrhea eventually leading to malabsorption and weight loss (22, 57). Crohn's is a life-long disorder leaving patients to endure unpredictable periods of relapse and remission. Because there is no cure, their quality of life can be severely compromised as a result of these recurring episodes (22).

Crohn's Disease Epidemiology: Incidence and Prevalence

Because most epidemiological studies to date have concentrated on specific regions or populations within a country, the full extent to which CD has reached cannot be completely grasped. However, these studies have defined certain attributes of the disease that provide clues to Crohn's etiology. For instance, Crohn's is a slow progressing condition primarily striking in a person's prime of life, most commonly between the ages of 15-40 years of age (22). Men and women are affected equally with the majority of cases reported in Northern Europe and North America (22, 15, 67). Some reports have demonstrated a possible heritable link among Crohn's patients, with 20-25% having a close relative with IBD, while others have pointed strictly to environmental agents as culprits of disease (74, 37). Although the ethnic and geographical distribution of the disease in the U.S. had not been extensively studied in decades past, Dr. Loftus, in 1997, did provide a glimpse into the prevalence of IBD in a report using information gathered by the Rochester Epidemiology Project (44). According to this unique records linkage system, 133 persons in 100,000 living in Olmsted County, Minnesota, suffer from Crohn's with 5.8 new cases in the same population every year. The results of this publication were based upon the Caucasian community with comparable numbers likely in African-American and Hispanic populations. Furthermore, people of Jewish heritage were found to be 4 to 5 times more likely to contract IBD than people in the general population. When these statistics were applied to the rest of the country, Dr. Loftus extrapolated that approximately 500,000 people have Crohn's in the U.S. (15, 44). Conversely, a group of pediatricians have shown through their two year study that children in Wisconsin contracted IBD with an incidence of 7.05 per 100,000. The distribution of disease was equal among all ethnic groups and geographical locales. The rate of

CD was nearly double that of Ulcerative colitis (UC) cases with 89% being non-familial incidences (37). Taken together, data collected from these recent studies supports the proposal that CD is a multi-factorial disease whose complete etiological spectrum is still emerging, with some cases involving an inherited component of susceptibility to environmental pathogens while others seem to be explained by unfavorable external conditions and exposure. According to Dr. Loftus, studies such as these that are concentrated to a particular area or region serve to limit a global understanding and picture of Crohn's epidemiology. Several factors may contribute to such diverse results in these epidemiological studies such as different methodologies employed as well as diverse genetic and environmental agents present in the different populations. Consequently, Dr. Loftus has proposed a national longitudinal database of Crohn's patients as a tool to better define the incidence, prevalence, and geographical distributions of disease (43).

Crohn's Disease Diagnosis and Methodology

CD can be difficult to distinguish as it is easily confused with other intestinal disorders. Consequently, an extensive physical exam and panel of blood tests may be required for accurate diagnosis. A low red blood cell count could indicate anemia, an evidence of bleeding in the intestines. Further, a high white blood cell count would signify a sure sign of inflammation in the body. A stool sample may also be helpful in determining intestinal hemorrhaging or infection. An upper GI will allow the small intestine to be checked for any obvious abnormalities. Before X-rays are taken, patients drink a white, chalky solution composed mainly of barium that coats the small intestinal lining. The white contrast of the barium reveals inflammation or lesions that may be present. To view the large intestine, the doctor may use an

endoscope, a light mounted at the end of a long flexible tube, to perform a colonoscopy at which time a biopsy may be taken for further analysis. The sampled tissue may be viewed under the microscope to confirm the level of inflammatory tissue involvement (57, 15). Ideally, immunological tests based upon sera cross-reactivity or DNA detection via PCR could clearly diagnose CD if associated with an infectious agent.

Crohn's Disease and Mycobacteria

The genus *Mycobacterium* contains over seventy validly named species with thirty-two known animal and human pathogens. All mycobacteria are aerobic, gram-positive, straight or curved, mesophilic bacilli. The non-motile rods are easily distinguished from other bacteria by their resistance to alcohol-mediated decolorization termed acid-fast positive (60). This classic mycobacterial feature is due to their thick, waxy cell wall composed primarily of mycolic acids and arabinose derivatives (24). Their genomes are GC-rich, about 59-66% of their total DNA content, and share very similar homology with few antigenic determinants (45, 1, 5). Mycobacteria can be assigned to two broad categories based on their reproductive growth rates. Most pathogens, like *Mycobacterium tuberculosis* complex and *Mycobacterium avium* complex (MAC), belong to the slow-growers requiring at least seven days to produce visible colonies on solid media under controlled conditions (45, 70). They survive mainly from host to host while a few species, including some MAC, survive in environmental reservoirs as the fast-growers. The MAC includes several subspecies including *M. avium* subspecies *avium* (MAV) *M. intracellulare* (MI), *M. avium* subspecies *silvaticum* (MAS), and *M. avium* subsp. *paratuberculosis* (MAP). Both MAV and MAP grow best on egg yolk and OADC supplemented

Middlebrook media at 37 ºC. However, they differ in that MAV will produce yellow colonies after seven days of incubation, whereas it can take 3-6 weeks to grow the whitish colonies of MAP. Another difference is that MAP is mycobactin-dependent, while MAV produces its own iron-chelating siderophore (20, 77). There are few genotypically distinct characteristics to separate the two subspecies. Recent genomic mapping and bioinformatics studies recognize three such differences among the MAC subspecies. MAP contains 14 to 18 copies of the IS900 insertion sequence, identifiable by PCR and Southern hybridization, a 6,496 bp single cassette responsible for biosynthesis of surface carbohydrate, and an additional 11kb section of DNA located in the IS900 element (68, 29, 5). Moreover, MAP is the confirmed inflammatory agent of JD in cattle and other ruminants, whereas MAV is considered an opportunistic pathogen, usually found in immuno-compromised patients (26, 28).

Crohn's Disease Etiology: Theories and Reality

Much debate concerning the etiology of CD has been argued in the scientific literature since Crohn re-distinguished it as a separate disorder in 1932. Everything from diet and environmental pathogens to autoimmunity and genetic aberrations have been implicated as playing possible roles in the pathology of Crohn's. Innovative research via new technologies is beginning to shed light on the true origins of Crohn's which may actually involve several etiological factors. This current research hypothesizes that acquiring CD is the result of a genetic predisposition that is exploited by an environmental trigger, namely a bacterial pathogen, causing an abnormal immune response (35, 8, 65, 23).

The Genetic Susceptibility Factor

In order to more clearly understand whether CD is an inherited or acquired disorder, many investigators have explored the familial occurrence of the disease. Scientists have discovered a greater than expected incidence for site and clinical type of CD within individual families. A pattern of young age onset and disease complications was also uncovered in correlated familial cases as compared to isolated incidences. These studies provide strong evidence that genetic factors are significant determinants of CD susceptibility and pathology (2). Statistical rates of disease in siblings and monozygotic twins further implicate a genetic contribution to acquisition of disease that is equivalent to other immune-mediated disorders such as multiple sclerosis and insulin-dependent diabetes (22, 62, 63). Several genetic loci have been analyzed as possible factors in the development of CD. One such recently discovered gene called NOD2/CARD15 may prove to be a catalyst for ground-breaking genetic and therapeutic advances. Located in the IBD1 locus on chromosome 16q12, it is thought to encode a disease resistance protein on monocytes, similar to anti-microbial proteins expressed in plants (58, 34, 59). NOD2/CARD15 belongs to a family of intracellular protein receptors called NBS-LRR (nucleotide-binding site; leucine-rich repeat) that have been demonstrated to recognize the peptidoglycan motif of bacterial pathogens by binding the MDP (muramyl dipeptide) component. Once activated by the bacterial cell wall, NOD2/CARD15 is capable of inducing NfkappaB, a key pro-inflammatory pathway responsible for the production of several immuno-regulators such as cytokines and chemokines (7, 78, 59). Further experimental data find that NOD2/CARD15 is upregulated by specific cytokines, namely TNF-alpha, thereby amplifying the immune response and facilitating a continuous cycle of inflammation (31, 61); the overexpression of NOD2/CARD15 seen in CD

patients serves to further explain this exaggerated immune response associated with Crohn's (3). A frameshift mutation in NOD2/CARD15, caused by a cytosine insertion, as well as several single-nucleotide polymorphisms have been shown to decrease the innate immune system's ability to recognize certain pathogens, particularly in cases of ileal CD versus colonic disease (16). This selective association is supported by the finding that the NOD2/CARD15 gene is found most abundantly in paneth cells, which are located primarily in the terminal ileum where they serve as a major host defense against gut microbes (40). Inherited defects in NOD2/CARD15 have been observed in 30-50% of CD patients compared to 7-20% of healthy controls (31). The fact that NOD2/CARD15 gene mutations have been positively correlated to the contraction of Crohn's provides one of the first physical links between an infectious agent and irregular immune response at the molecular level (58, 31).

Why is *Mycobacterium* a Good Candidate for Crohn's Disease Pathogenesis?

The remarkable similarities between CD and other well-documented mycobacterioses in humans and animals have kept researchers returning to the theory that CD has its etiology rooted in mycobacterial infection (74, 20, 42, 9, 29, 32, 13, 54, 26). The parallels between CD and JD remains one of the best arguments for this hypothesis. The pathology and symptoms of Johne's or bovine paratuberculosis infection was first described as early as 1806 by Professor Edward Skellet in his book entitled Parturition of the Cow (38). However, it was Johne and Frothingham who are said to have first documented these symptoms as a disease by demonstrating a link between mycobacteria and paratuberculosis in ruminants (73).

Upon receiving the tissues of a cow, from a local German farmer, thought to have succumb to intestinal tuberculosis, Johne and Frothingham performed a histological examination where they found an abundance of immune cells in the abnormally thick, intestinal mucosa and wall including leukocytes and epitheliod cells. Acid-fast staining and microscopic evaluation of the ruminant intestine revealed colonies of acid-fast micro-organisms similar to *Mycobacterium bovis,* the bacteria that causes tuberculosis in cattle. Because the sample failed to cause disease in guinea pigs, Johne classified the discovery as *Mycobacterium avium,* the pathogen responsible for tuberculosis in birds (73). Today, scientists have further typed that organism more specifically to MAP.

The connection between these histologically inseparable disorders is strengthened by evidence that Johne's may be easily transmitted to cattle and other mammalian populations including humans (29). Originally considered a disease strictly affecting dairy cows, Johne's is most prevalent in cattle with approximately 40% of all U.S. dairy herds containing at least one infected animal. Calves are often infected through their mother's colostrum and milk (69). However, Johne's may be spread via the fecal/oral route to other species including sheep, pigs, goats, and horses. Once mycobacterial exposure and colonization occur, infection originates in the Peyer's patches where gut pathogens are absorbed through M cells to be phagocytized by macrophages. Due to their thick, waxy cell wall, the mycobacteria are able to evade degradation in the phagolysozome normally caused by low pH molecules like nitric oxide. Consequently, the pathogens thrive undetected perpetuating the infection and risk of transmittance (51, 72).

Furthermore, there is compelling data to suggest that the parasitic mycobacteria that cause Johne's can be disseminated throughout the human food chain. Several studies testing thermal tolerance of mycobacterial species concluded that several *M. avium* subspecies including *paratuberculosis* are capable of penetrating the dairy supply by surviving the pasteurization process (29, 45, 8, 25, 48). The pathogenic organisms persist by migrating to the cow's udder within protective leukocytes where they directly contaminate excreted milk. Ground beef as well as dairy can be considered a potential source of human exposure to infectious mycobacteria, especially since most animals are slaughtered or milked before the manifestation of disease. Ground water contamination is yet another means of possible animal to animal or animal to human transmittance (8, 22). Surface waters which feed into domestic water supplies often contain agricultural waste runoff. Studies have revealed that *M. avium* is not eliminated by common water treatment practices which include filtration and chlorination (22, 8, 29).

Pathological comparison of CD to other mycobacterial diseases, namely tuberculosis and leprosy, provide additional credibility to the notion that CD etiology is directly linked to the mycobacterial family. The progression of CD symptoms manifest extremely similar to that of tuberculosis. Often Crohn's and intestinal tuberculosis have indistinguishable pathologies, only characterized by specific molecular typing via polymerase chain reaction and acid-fast staining. Mycobacterial disease usually presents in two major forms: contained or aggressive. A contained or tuberculoid/non-perforating response to infection is described mainly by the presence of granulomas that eventually lead to chronic intestinal obstruction (35, 49). The aggressive or perforating form is characterized by severe ulcerations in the intestinal wall that

advances to fistulas, abnormal connections or pathways between sections of bowel. Both of these forms have been documented in Crohn's patients and sometimes display a “dual presentation.” The spectrum of acquired symptoms is thought to be based upon a patient's cell-mediated immune response to pathogenic mycobacterial antigens, suspected to be an inherited trait (35).

Success in treating Crohn's with a cocktail of anti-mycobacterial drugs gives even further evidence that CD can be ascribed to mycobacterial infection. Macrolide antibiotics are essential in treating most mycobacterial diseases due to their ability to penetrate macrophages and metabolizing immune cells thereby eradicating the intracellular pathogens (9, 46). These medications which include clarithromycin and azithromycin need to be administered in combination with other macrolide drugs like rifabutin, a common anti-tuberculosis treatment, in order to combat the phenomenon of multi-drug resistance. For instance, in 1997 Hermon-Taylor's study of 52 diagnosed Crohn's patients demonstrated a 93.5% clinical remission rate after treatment with rifabutin in combination with clarithromycin or azithromycin for six months. Many patients maintained remission status with no symptoms for up to two years depending upon the severity of prior disease (27).

The Host Immune Response

Some proponents still debate mycobacteria as the true etiology of CD based upon the ambiguity surrounding the current evidence of a specific immune response to MAP in CD patients. It is clear that most Crohn's sufferers demonstrate a much different and unexpected immune reaction

as compared to victims of many other infectious agents (18, 35). The anergic immune reactions demonstrated in CD patients are driven by an elevated Th1 cytokine profile, including IL-12 and INF-gamma, (4) that induces a damaging type of chronic inflammation as opposed to Th2 cytokines that promote a healing immune response (9, 39). However, several pathogenic micro-organisms have been identified, including *Mycobacterium tuberculosis* and *Mycobacterium leprae*, that have evolved sophisticated measures to circumvent the human immune system producing similar dysregulated immune responses (35). For instance, as intracellular parasites, the microbes that comprise the *Mycobacterium* family target and inhabit macrophages, the primary immune cells responsible for destroying invading bacteria. By resisting degradation in the phagolysozome, the bacteria are able to avoid normal antigen presentation, thereby creating a type of pathogenic "sanctuary" where they can thrive protected from the threat of other immune cells (30). Other mycobacteria species, like *M. leprae*, actually impede the actions of the cell-mediated immune response by suppressing the production of cytokines in the host (71). Still, some bacterial species possess antigenic epitopes strikingly similar to that of host molecules. These shared components can elicit a perpetual molecular mimicry state, analogous to the mechanisms of autoimmunity, whereby bacterial antigens appear as self antigens, thus escaping detection by the immune system. This phenomenon has been investigated concerning mycobacterial heat shock proteins and outer envelope polysaccharides due to their homology to human epitopes. However, concrete evidence of molecular mimicry in these cases has yet to be established (35, 19, 41). Moreover, antigen-antibody investigations into the Crohn's immune response may be hampered by sero-cross reactivity caused by the many shared antigens among species of mycobacteria. Some pathogenic mycobacteria have up to a 65% cross-reactivity rate

as a result of such close homology between their antigens (18, 35). Consequently, statistical results concerning control groups versus test subjects can be skewed by patients unknowingly exposed to different mycobacterial organisms (9, 75). Therefore, it is imperative to discover immunogenic antigens that are specific to MAP in order to more thoroughly study the potential of a mycobacterial etiology associated with CD. It is bacterial survival strategies such as these coupled with other determinants such as the genetic make-up of the host and organism and environmental factors that serve to cloud a definitive understanding of the immuno-modulatory responses that are initiated by mycobacterial infection.

Spheroplast Versus Bacillary

CD has long been suspected of having an etiological relationship to mycobacteria, ever since its recognition as a distinguishable condition in the early twentieth century. However, attempts by researchers to establish a link between CD and mycobacteria proved frustrating after continual failures to isolate and culture acid-fast bacilli from infected Crohn's tissue. But, when Chiodini et. al. were the first to isolate an unclassified mycobacterial species from three Crohn's patients in 1984, enthusiasm was again sparked in the scientific community concerning a plausible connection between CD and mycobacteria (9, 10, 11). With this success came new insights into the prior inability of investigators to detect mycobacteria in Crohn's tissue. Chiodini soon found that these primary isolates lacked a definitive cell wall only reverting to bacillary form after months of incubation on supplemented media. Restriction polymorphism techniques revealed the genetic identity of these bacteria as MAP (9, 10, 12). It is now understood that MAP survives in two states: spheroplast and bacillary forms. Current theories postulate that MAP becomes an

invasive human pathogen in its spheroplast form as opposed to the bacillary form that infects ruminants (9, 33). Spheroplasts are characterized by a partial loss of cell wall with resistance to acid-fast staining, increased sensitivity to osmotic pressures, and dependence on iron-scavenging compounds such as mycobactin. Several genes specific to MAP are now thought to regulate the expression, modification and transfer of the sugar fucose to cell wall GPL's (glycopeptidolipids). These oligosaccharide moieties coating the cell may contribute to the bacteria's ability to adopt an acid-fast and protease resistant, non-bacillary form (68, 66). Attributes such as these combined with harsh processing techniques used in mycobacteriology, which can damage the exposed cell membrane, further complicate culture and subsequent identification of MAP in Crohn's tissue. Even if proper growing conditions are met, identification of MAP depends upon the spheroplast achieving an intact cell wall with recognizable morphology, which can take several months to a year decreasing the probability of recovering viable organisms (9, 47, 35). The presence of spheroplasts may explain the limited immune response observed in most CD patients. Cell wall deficient bacteria often have poor immunogenic properties due to diminished envelope epitopes but retain the ability to evoke a local hypersensitivity reaction seen in chronic CD (35).

Variability in Laboratory Techniques

The multi-faceted complications associated with the detection of MAP in CD tissue can serve to undermine the logical correlation of mycobacteria to this intestinal disorder if not properly assessed. MAP had eluded the most erudite scientists for decades until Chiodini discovered ground-breaking information in the 1980's concerning its nature and requirements for tissue

culture (10). Similarly, researchers are beginning to recognize and correct the reasons behind years of inconsistent experimental results concerning MAP detection in CD. The understanding that MAP may be present in different distributions and forms throughout diseased tissue may be the key to unlocking the variability observed in the efficiencies of several laboratory detection techniques. For instance, in animals, JD is seen in a pluribacillary or paucibacillary form with little to no MAP detected in the latter (35). This may extend to humans whereby spheroplasts are often sparsely scattered throughout CD tissue making them difficult to recover. The efficiency of DNA extraction is imperative in the detection of MAP in CD tissues. The lack of adequate spheroplasts coupled with different extraction methods have proven to dramatically affect MAP detection. The preparation of experimental tissue has also been recently called into question. Traditional paraffin-mounted tissue has shown to contain inhibitors that interfere with PCR amplification of MAP (77). Furthermore, different PCR reagents and protocols range in their sensitivities for the amplification of certain mycobacteria fragments (27). The development of laboratory techniques that address these complications to better identify mycobacterial species in diseased tissue is, therefore, essential in establishing the foundation of Crohn's etiology.

Rationale and Objectives

Data supporting the role of MAP in CD etiology is mounting, yet there is still considerable skepticism regarding the role that MAP or MAP-like organisms may play in this disease. Therefore, consistent protocols that accurately conclude the presence or absence of MAP in specimens from CD patients are urgently needed. The recent introduction of Bactec and MGIT enriched liquid culture systems and IS900 specific PCR assays have greatly improved MAP

detection. However, the transposable IS900 element has been found in other *Mycobacterium* species in co-infected patients, such as those with IBD and HIV, which suggests that still more approaches are required to enhance the specificity and sensitivity of MAP detection in Crohn's tissue. The close homology of MAC subspecies and the possibility of IS900 lateral transfer to other MAP-like derivatives underscores the importance for the accurate identification and study of epidemiological versus geographical distributions of MAP (53). In an attempt to investigate the role of mycobacteria in IBD, especially CD, the objectives of this study were as follows: 1) to culture MAC and/or MAP from Crohn's biopsied tissue, 2) to design a sensitive, efficient PCR protocol for the detection of MAC in CD tissue, 3) to identify a library of mycobacterial isolates through molecular typing techniques, 4) to evaluate a set of representative DNA sequences in order to investigate homological and epidemiological differences among isolates. It is hoped that the outcome of this study will guide future endeavors toward better approaches when investigating the mycobacterial role in Crohn’s disease etiology and epidemiology.

MATERIALS AND METHODS

Specimen Processing

Specimen Collection and Logging

The full thickness surgical tissues used in this study were kindly collected and shipped to the University of Central Florida by collaborators at Mt. Sinai hospital in New York. The tissue samples were cataloged blindly and referred to only by their assigned code (ex. MS1, MS2, MS3, etc.). All reference information including dates of arrival and processing were recorded. The specimens were packaged on ice and received cold but not frozen. Normal tissue and inflamed tissue specimens from each subject were collected if possible. Figure 1 shows the form that was used to document each incoming sample.

Homogenization and Decontamination

All tissue samples were processed within a class II Biosafety facility. Proper laboratory attire, such as latex gloves and a laboratory coat, were worn at all times to ensure the safety of the laboratory environment and the integrity of each specimen. Samples arriving to the laboratory were immediately unpacked, removed from ice, and transferred from their sterile glass vial containers to a fresh 50 mL centrifuge tube. The tissue was then placed into a disposable 50 mL

tissue grinder until completely homogenized. The ground tissue was decontaminated to eradicate all extracellular organisms by the addition of 5 mL of BBL MycoPrep NALC-NaOH (n-acetyl-L-cysteine-NaOH) solution. The centrifuge tube containing the MycoPrep/tissue mixture was vortexed for 1 minute and allowed to set at room temperature for 20 minutes, with intermittent swirling. The final volume of the mixture was brought up to 50 mL with phosphate buffer solution (PBS, NA2HPO4, KH2PO4, pH 6.8) followed by centrifugation at 3,000 rpm for 20 minutes at room temperature. The supernatant was discarded, and the pellet was washed twice in 1 mL of PBS at 10,000 rpm at 4^{o} C before being suspended in a final 1 mL volume of PBS (64, 55).

Figure 1. Documentation and Tracking Form for each Tissue Received.

Serial No. .....

TEST REQUEST

Patient Code: _____

Date of Collection: _____

Date of Arrival/UCF: _____

Condition (circle): **Cold** **Frozen** **Room temp.**

Specimen

	Whole Blood	Serum	Tissue
(check one)	☐	☐	☐

Comments

_____

_____

_____

Picked up by _____

Culture and Growth Condition

A 0.5 mL portion of each homogenized, decontaminated tissue specimen was aseptically inoculated into two types of supplementally enriched, liquid media specific for the growth and support of mycobacteria as follows:

The Bactec Culture System

Bactec 12B Mycobacteria liquid culture Media works as part of a system of mycobacterial growth detection in conjunction with the Bactec 460TB Reader. The basic medium consists of Middlebrook 7H9 broth as a base with the addition of catalase, casein hydrolysate, bovine serum albumin, and ^{14}C labeled palmitic acid. The media was enriched with several types of supplements to further support the cell wall growth of MAC, in particular the elusive membrane of subspecies *paratuberculosis*. These include 0.5 mL of BBL OADC, which contains oleic acid, bovine albumin, dextrose, and catalase; 0.1 mL BBL Panta broadspectrum antibiotic cocktail which includes polymixin B, amphotericin B, nalidixic acid, trimethoprim, and azlocillin; and 0.016 mL Mycobactin J (2 mg/L), an iron chelator molecule. Furthermore, a duplicate Bactec culture was prepared for each sample that contained all previously mentioned ingredients with the addition of 1 mL Bacto 50% Egg Yolk Enrichment (Difco) to further enhance mycobacterial cell wall synthesis. All aseptically inoculated Bactec culture bottles were then incubated in a 5% CO_2 incubator at a constant 37^{o} C. Approximately every three to five days from the date of inoculation, the Bactec culture bottles were placed into the automatic

Bactec 460 TB analyzer to measure the amount of ^{14}C labeled CO_2 emitted by the mycobacterial organisms during growth. (64, 55)

Bactec 460 TB Growth Detector

Inoculated mycobacteria that grow within the Bactec 12B vial utilize provided nutrients, especially ^{14}C labeled palmitic acid, in order to synthesize new cell wall as they divide. The expanding population of organisms emits $^{14}CO_2$ as a by-product of respiration that is proportional to the level of cell division and is measured by the Bactec analyzer as growth index. Determination of a sample's growth index begins once the vials are loaded sequentially into the Bactec reader. First, however, a standard Bactec bottle containing a pre-determined volume of $^{14}CO_2$ is initially used to calibrate the instrument. The CO_2 gas by-product is drawn from the Bactec bottle by a sterile needle attached to a robotic arm. Once aspirated into the needle, the CO_2 is pushed through the system into a CO_2 trap as a result of surrounding air being drawn into the needle through a dust filter and into the ion chamber via a flush valve. The electrometer is thus cleaned and ready for the next sample in the cycle. When two 18G needles are heated, the robotic testing needle is driven through the rubber septum of the test vial provided by the manufacturer (Becton-Dickinson). Extracted $^{14}CO_2$ from the sample is drawn into the ion chamber by a pump-driven vacuum. The radioactively labeled CO_2 present in the given sample creates a tiny electric current which is detected by the electrometer in the ion chamber. This current is then magnified and displayed as the sample's growth index (GI). The labeled CO_2 used to measure cell growth in an individual vial is replaced by a volume of fresh 5% CO_2 to continue the promotion of mycobacterial growth in the Bactec bottle. The growth index is measured

according to a scale of 0, meaning no detected growth, to 999, indicating maximum level of microbial activity. Samples registering a GI of 10 or greater, a threshold a positive growth, are usually returned to the incubator to allow more time for advancement. Vial contents that give a reading of 999 are harvested, with a portion inoculated into fresh Bactec media. Figure 2 shows illustration of the Bactec 460 TB analyzer.

The MGIT (Mycobacterial Growth Indicator Tube) culture system

The MGIT system uses an oxygen-sensitive growth indicator that fluoresces as oxygen levels decrease due to bacterial respiration. This non-radioactive compound, Tris 4,7-diphenyl-1,10-phenanthroline ruthenium chloride pentahydrate, is inlaid in a rubber matrix at the bottom of the media test tube. Mycobacterial growth may also be determined as the result of turbidity in the MGIT vial. The basic media consists of Middlebrook 7H9 broth, casein peptone, glycerol, and 5% CO_2. The MGIT growth media was supplemented with the same substances as the Bactec media excluding the egg yolk. The aseptically inoculated MGIT tubes were evaluated for bacterial growth approximately six weeks from the date of inoculation after incubation in the same 5% CO_2 incubator at 37^{o} C (64, 6, 55).

Figure 2. Photograph and Schematic Diagram of the Bactec 460 TB Analyzer.

(A) Photograph of Bactec System in Biomolecular Building, Room 221.
(B) Image of Bactec Analyzer Diagram was obtained from the Becton-Dickinson Operating Manuel.

A.

B.

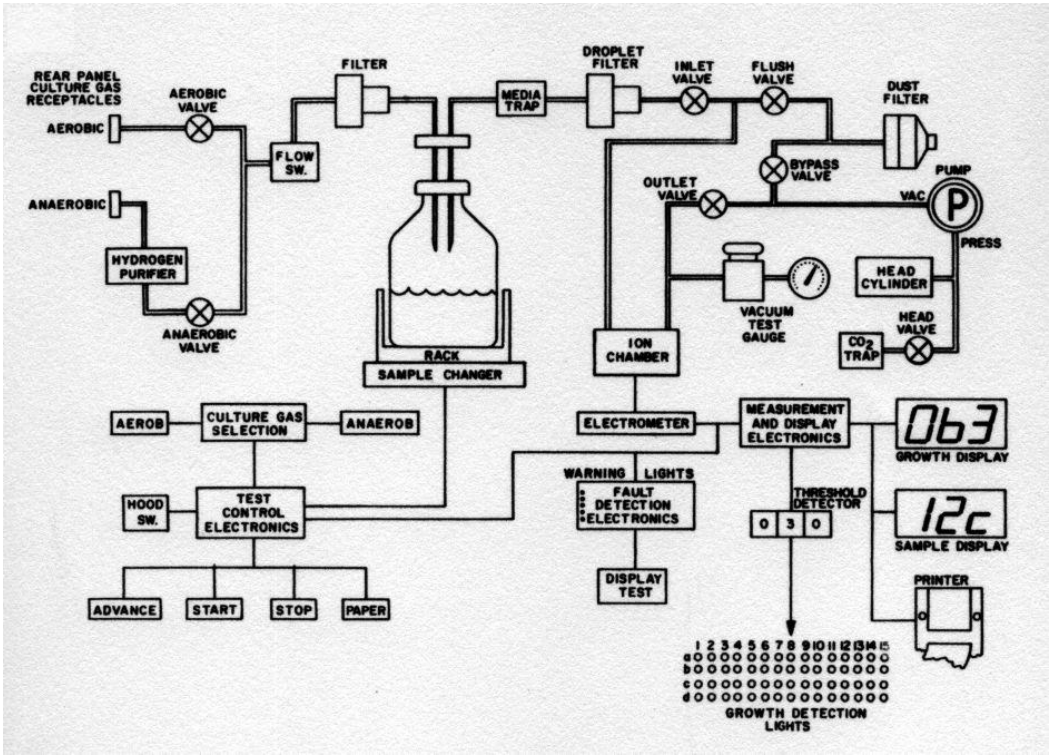
REAR PANEL CULTURE GAS RECEPTACLES
AEROBIC
ANAEROBIC
AEROBIC VALVE
ANAEROBIC VALVE
HYDROGEN PURIFIER
FLOW SW.
FILTER
MEDIA TRAP
DROPLET FILTER
INLET VALVE
FLUSH VALVE
DUST FILTER
BYPASS VALVE
OUTLET VALVE
PUMP
VAC
PRESS
HEAD CYLINDER
HEAD VALVE
VACUUM TEST GAUGE
CO2 TRAP
ION CHAMBER
RACK
SAMPLE CHANGER
AEROB
CULTURE GAS SELECTION
ANAEROB
HOOD SW.
TEST CONTROL ELECTRONICS
ADVANCE
START
STOP
PAPER
ELECTROMETER
MEASUREMENT AND DISPLAY ELECTRONICS
063
GROWTH DISPLAY
WARNING LIGHTS
FAULT DETECTION ELECTRONICS
THRESHOLD DETECTOR
0 3 0
12c
SAMPLE DISPLAY
DISPLAY TEST
PRINTER
1 2 3 4 5 6 7 8 9 10 11 12 13 14 15
a
b
c
d
GROWTH DETECTION LIGHTS

Subculture Media

Once a maximum growth reading of 999 using the Bactec system or visible turbidity using the MGIT system was determined in a particular culture, the sample was then subcultured on solid media in an attempt to isolate and visualize the morphology of specific mycobacterial colonies. After thorough vortexing of the sample to be subcultured, a sterile loop was used to aseptically transfer the positive culture broth onto a Mycobactosel L-J Medium Slant (Becton-Dickinson) with the following formula of reagents dissolved in 600 mL of purified H_20: 2.5 g Monopotassium Phosphate, 0.24 g Magnesium Sulfate, 0.6 g Sodium Citrate, 3.6 g L-Asparagine, 30.0 g potato flour, 0.4 Malachite Green, 0.64 g Cycloheximide, 0.0032 g Lincomycin, 0.056 g Nalidixic Acid, 12 mL Glycerol, and 1000.0 Whole Egg. The slants were then supplemented with 100 uL of Mycobactin J (2mg/L) to promote the growth of siderophore-dependent *Mycobacterium* species. The subcultures were stored at room temperature for 6-8 weeks or until detectable colonies appeared, after which the bacteria were harvested for analysis.

Genomic DNA Extraction

All MGIT, Bactec, and subcultured samples that showed positive growth were subjected to genomic DNA extraction by the boil method using Phase-Lock Gel tubes. After vortexing, a 100 uL portion of each sample was removed aseptically with a sterile syringe or loop and placed into a clean 1.5 eppendorf microcentrifuge tube. Each tube was then centrifuged at 14,000 rpm for 10 minutes at 4^o C. The supernatant was discarded, and the pellet was resuspended in 100 uL of TE

buffer (10 mM Tris and 1 mM EDTA, pH 8.0 HCL). The samples were boiled for 30 minutes at 100° C in a dry heat bath followed by an immediate 15 minute ice bath at 4° C. After centrifugation of each sample at 12,000 rpm for 10 minutes at 4° C, the supernatant was transferred to a prepared Phase-Lock Gel tube containing 200 uL of phenol/chloroform/isoamylalcohol. The aqueous sample and organic solution in the Phase-Lock Gel tube were mixed thoroughly without vortexing until a homogeneous suspension was achieved. The Phase-Lock Gel tubes were then centrifuged at 12,000 rpm for 5 minutes at 4° C, after which the upper aqueous phase containing the genomic DNA was transferred into a new 1.5 mL eppendorf microcentrifuge tube. The samples were incubated overnight at -20° C in 200 mL of cold 100% ethanol. Following precipitation, the samples were again centrifuged at 14,000 rpm for 20 minutes at 4° C. After the 100% ethanol was pipetted off and discarded, the DNA pellet was washed with 400 uL of 80% ethanol; the tubes were re-centrifuged at 14,000 rpm for an additional 20 minutes at 4° C. Finally, the 80% ethanol was removed, and the DNA pellet was dried in a DNA speed vacuum for 5 minutes and re-constituted in 50 mL of sterile, filtered qH_2O. Each extract was stored at -20° C. (64, 55)

PCR Analysis

The Oligonucleotide Primers

Each DNA extract was evaluated by a PCR panel in order to detect and distinguish between *Mycobacterium avium* subspecies: *avium*, *paratuberculosis*, and *intracellulare*. Oligonucleotide

primers A-16-R (5'-ACCAGAAGACATGCGTCTTG-3') and A-16-L (5'-AGAGTTTGATCCTGGCTCAG-3') specific for the amplification of the 193 base pair 16S rRNA internal spacer region were used to detect the presence of subspecies *avium* and *paratuberculosis*. Primers MAC-R (5'-AGGTGGCGTCGAGGAAGAC-3') and MAC-L (5'-GCCGCCGAAACGATCTAC-3') were used to identify the 427 base pair insertional sequence 1245 indicative of the MAC which contains all of the above mentioned subspecies. Two specific primers P90 (5'-GTTCGGGGCCGTCGCTTAGG-3') and P91 (5'GAGGTCGATCGCCCACGTGA-3') were employed as part of a PCR duplex reaction to determine the presence of the 401 base pair insertional sequence 900 array specific to the *paratuberculosis* genome. The second round of DNA amplification required primers Av1 (5'-ATGTGGTTGCTGTGTTGGATGG-3') and Av2 (5'-CCGCCGCAATCAACTCCAG-3') to increase the copy number of a 298 base pair internal region of the IS900 paratuberculosis sequence. All oligonucleotide primers used in this study were sequenced by Qiagen. Lypholized primers were dissolved in 100 uL of sterile TE buffer (10mM Tris and 0.1 mM EDTA, pH 7). Table 1 summarizes all of the oligonucleotide primer sequences utilized in this study (64, 6, 55, 21).

Optimization of the PCR Condition

The amplification of each desired target sequence, including the 16S rRNA, IS1245, and IS900 regions, was optimized by following a series of crucial steps to achieve the highest possible number of amplicons. The process began by calculating the best temperatures at which to anneal the primers to complementary genomic DNA sequences. This was done by computing the

melting temperatures from which the annealing temperatures were determined, using the following two equations: Tm = [(#A + T) x 2°C] + [(#G + C) x 4°C] and Ta = Tm – 5°C. Next, the number and time of extension cycles were estimated based upon the length of the fragment being copied (76). Finally, the optimal PCR reagent concentrations along with the DNA template amounts were deduced by a battery of trial and error experiments. The specific PCR reaction ingredients that were scrutinized include, oligonucleotide primers, Taq DNA polymerase, as well as, DNA co-solvents $MgCl_2$ and betaine. Due to the similar nucleotide content of each primer set and length of the target fragments, one protocol allowed maximum detection for each desired sequence.

PCR Controls

All PCR experiments included two negative controls of sterile TE buffer (10 mM Tris and 0.1 mM EDTA, pH 8) to certify the absence of contamination in both the PCR reactions and the genomic DNA extraction process. Appropriate positive controls were also used for sample comparison that included extracted *avium* and *paratuberculosis* subspecies DNA. Positive control DNA and PCR reactions were extracted and prepared separately to avoid contaminating the study samples.

Agarose Gel Electrophoresis Analysis

Once amplification was completed, the individual PCR products were visualized by electrophoresis. The expected fragment sizes from the four PCR assays ranged from 193 bp to 427 bp (see Table 1); therefore, a 2% g/v agarose gel containing 0.5 ug/mL ethidium bromide

dissolved in TE buffer (0.089 M Tris, 0.089 M boric acid, 0.002 M EDTA) was used for analysis. Specifically, 3 grams of agarose (Fisher Scientific) was added to 150 mL of TE buffer and heated in the microwave until completely dissolved. The mixture was then incubated in a water bath at 56° C for 20 minutes. Afterwards, a 3 uL volume of ethidium bromide was thoroughly mixed into the agarose solution before it was poured into a tray. The gel was allowed to incubate at room temperature for 30 minutes until completely polymerized. A 1.5 uL aliquot of 6x Blue/Orange Loading Dye containing glycerol and sucrose (Promega) was pipetted into a 20 uL volume of each PCR product and mixed. An additional 1.5 uL of loading dye was added to 4 uL of 100 bp DNA Step Ladder (Promega) or Low Mass DNA Ladder (Invitrogen) for fragment size comparison. The gel was then loaded with 21.5 uL of each DNA/dye mixture and 5.5 uL of the reference DNA/dye mixture. Electrophoresis analysis was performed at 120 volts for 30-40 minutes, and the resulting gel was documented and photographed using the Gel-Dock System (Biorad).

Microscopic Analysis

All subcultured samples and selected MGIT and Bactec cultures suspected of microbial growth were analyzed for the presence of mycobacteria by using the Ziehl-Neelsen method (Difco). The surface of each slant was gently scraped with a sterile loop and the residue placed in a 250 uL volume of qH_2O. A 50 uL aliquot of each microbial culture was then smeared onto a clean microscope slide and allowed to air dry. Once completely dry, the slides were quickly heat fixed over an open flame and cooled to room temperature. The slides were flooded with carbol-fushin for 10 minutes while exposed to a steam bath to allow maximum penetration of dye into the

bacterial cell wall. They were then rinsed with a continuous stream of acid alcohol reagent for 30 seconds followed by a distilled water wash. Malachite green was used as a counterstain to cover the slides for 1 minute before a final distilled water rinse. Afterward, the glass slides were gently blotted with bilbous paper and air dried prior to microscopic analysis. (64, 55) Slides displaying acid-fast positive bacteria were then photographed as the example in Figure 5 Illustrates.

DNA Purification

PCR products that yielded positive results for the presence of MAP after amplification using Av_1 and Av_2 primers were directly purified using the Wizard PCR preps DNA Purification System (Promega). This process was necessary for later DNA sequencing. According to this protocol, the P_{90} and P_{91} products that corresponded to positive Av_1 and Av_2 samples were amplified in duplicate until at least 30-300 uL of PCR reaction was obtained. The PCR product was then combined into one tube to which an aliquot of 100 uL of direct PCR purification buffer was added. The tube was thoroughly mixed. One mL of resin was combined with the PCR product/buffer solution and briefly vortexed three times over a one minute interval. A Wizard mini-column was prepared for each sample to be purified by removing the plunger from a 3 mL Luer-Lok syringe (Becton-Dickinson) and attaching a mini-column to the syringe barrel. The resin/DNA mixture was transferred from the tube into the syringe, and the slurry was gently pushed into the mini-column after insertion of the plunger into the syringe barrel. A fresh barrel was attached to the mini-column to which 2 mL of 80% isopropanol was added. The wash solution was slowly driven through the mini-column again with the original plunger. The syringe barrel was removed, and the mini-column was centrifuged in a 1.5 mL microcentrifuge tube at

12,000 rpm for 2 minutes at 4° C. The purified DNA was eluted into a fresh 1.5 mL microcentrifuge tube by pipetting 50 uL of sterile TE buffer directly onto the mini-column. After one full minute, the purified DNA was collected when the mini-column/microcentrifuge tube combination was centrifuged at 12,000 rpm for 20 seconds at room temperature. The mini-column was then discarded, and the DNA stored at –20° C until time of sequencing.

DNA Quantification

Following purification, the IS900 DNA amplicons were quantified using the DNA Dipstick Kit (Invitrogen) prior to being sent for sequencing. In house analysis revealed that the DNA Dipstick Kit results were comparable to spectrophotometer readings. The quantification procedure began by spotting 1 uL of purified DNA onto the dipstick membrane where it was allowed to completely air dry. The DNA dipstick containing the dry sample was then placed for 10 seconds into a provided cuvette containing 1 mL of wash solution. Next, the DNA dipstick was transferred to a second cuvette for 3 minutes which held 1 mL of coupling solution. The DNA dipstick was removed from the second cuvette and rinsed with deionized water for 20 seconds followed by a 4 minute incubation in the wash solution. A third cuvette was prepared that contained a solution of 1 mL developer stock and 1 drop of developer. The DNA dipstick was placed in the developer for 2 minutes and then gently rinsed in wash solution for 20 seconds. Finally, the DNA dipstick was laid flat, membrane face-up, to air dry. Once completely dry, the sample spot on the DNA dipstick membrane was compared to the color intensities of the control DNA spots on the standard chart reference card provided by the DNA Dipstick kit. The control

spots ranged in concentration from 0.1 ng/uL to 10 ng/uL; the sample concentrations were estimated based upon their closeness in color to the standard spots.

DNA Sequencing and Analysis

The PCR product containing the target DNA amplicon, a 298 base-pair internal region of the IS900 gene, resulted from a nested PCR assay (P90, P91 & Av1, Av2 primer sets). Figure 3 illustrates the amplified regions of the IS900 gene following nested PCR using the above mentioned primers. Once the required 30-300 uL volume of PCR product was obtained, it was purified directly by the Wizard PCR Preps DNA Purification System (Qiagen) previously described. The presence of the purified IS900 product was confirmed by agarose gel electrophoresis and quantified via the DNA dipstick and Low Mass DNA marker (Invitrogen). DNA sequencing of the different purified IS900 fragments was performed at the DNA Sequencing Core Facility in the Department of Molecular Biology and Microbiology at the University of Central Florida using the Av1 oligonucleotide primer sequence (Table 1). Raw nucleotide sequence data was analyzed using computer facilities at the University of Central Florida able to access the National Center for Biotechnology Information (NCBI) website (http://www.ncbi.nlm.nih.gov/). This particular internet site employs the *Entrez* search engine which can retrieve and compare data from many different databases that include such information as nucleotide sequences, protein sequences, whole genomes, macromolecular structures, and MEDLINE. The IS900 sequences acquired in this study were entered into the BLAST program, a comparative analysis tool provided via the world wide web, where they were

scrutinized against sequences in the NIH genetic sequence database also known as GenBank. (56)

Figure 3. Illustration of Amplified Regions of the IS900 Gene following Nested PCR using Primer Sets P90/P91 and Av1/Av2.

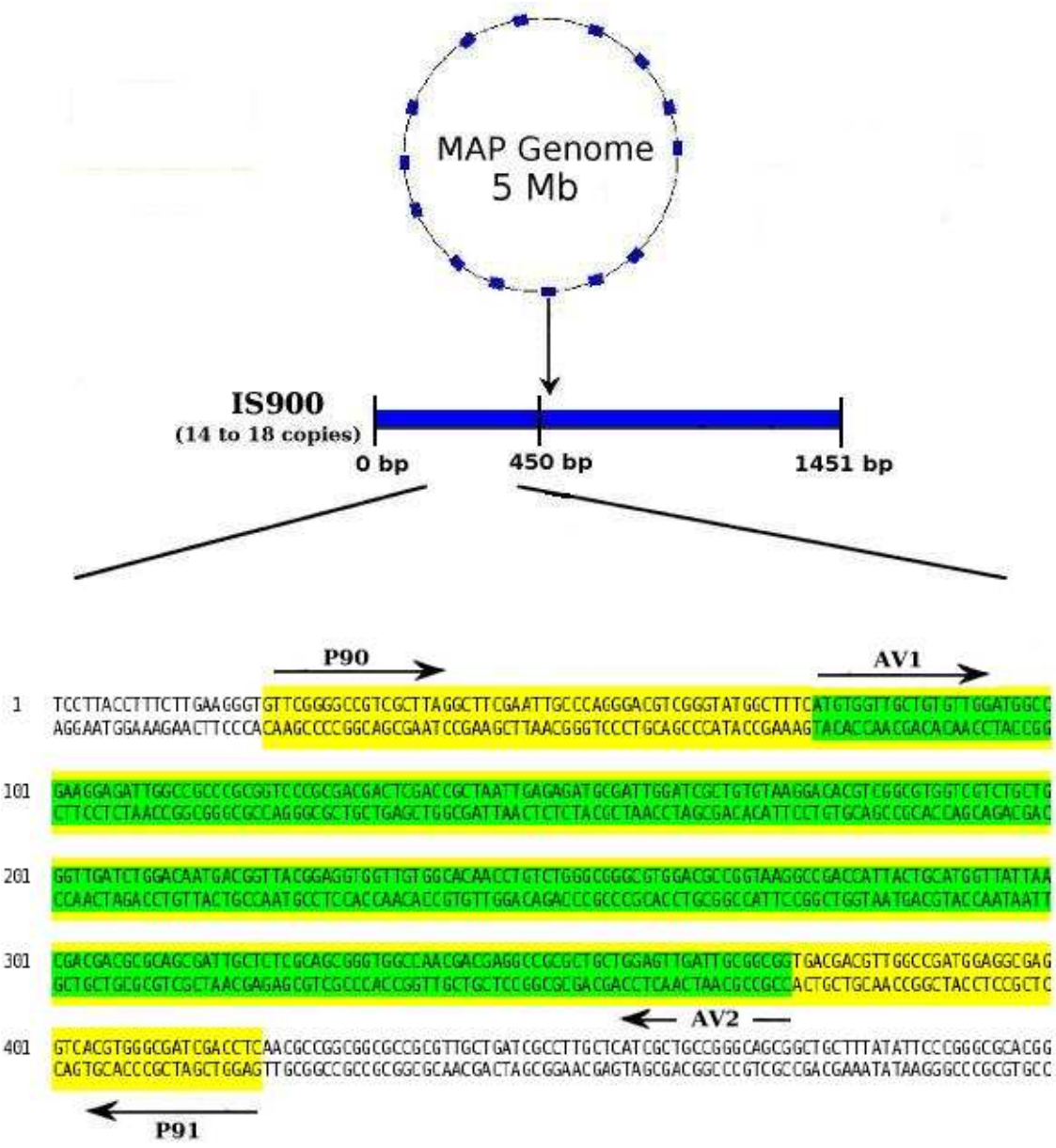
MAP Genome
5 Mb
IS900
(14 to 18 copies)
0 bp
450 bp
1451 bp
P90
AV1
1 TCCTTACCTTTCTTGAAGGGTGTTCGGGGCCGTCGCTTAGGCTTCGAATTGCCCAGGGACGTCGGGTATGGCTTTCATGTGGTTGCTGTGTTGGATGGCG
AGGAATGGAAAGAACTTCCCACAAGCCCCGGCAGCGAATCCGAAGCTTAACGGGTCCCTGCAGCCCATACCGAAAGTACACCAACGACACAACCTACCGG
101 GAAGGAGATTGGCCGCCCGCGGTCCCGCGACGACTCGACCGCTAATTGAGAGATGCGATTGGATCGCTGTGTAAGGACACGTCGGCGTGGTCGTCTGCTG
CTTCCTCTAACCGGCGGGCGCCAGGGCGCTGCTGAGCTGGCGATTAACTCTCTACGCTAACCTAGCGACACATTCCTGTGCAGCCGCACCAGCAGACGAC
201 GGTTGATCTGGACAATGACGGTTACGGAGGTGGTTGTGGCACAACCTGTCTGGGCGGGCGTGGACGCCGGTAAGGCCGACCATTACTGCATGGTTATTAA
CCAACTAGACCTGTTACTGCCAATGCCTCCACCAACACCGTGTTGGACAGACCCGCCCGCACCTGCGGCCATTCCGGCTGGTAATGACGTACCAATAATT
301 CGACGACGCGCAGCGATTGCTCTCGCAGCGGGTGGCCAACGACGAGGCCGCGCTGCTGGAGTTGATTGCGGCGGTGACGACGTTGGCCGATGGAGGCGAG
GCTGCTGCGCGTCGCTAACGAGAGCGTCGCCCACCGGTTGCTGCTCCGGCGCGACGACCTCAACTAACGCCGCCACTGCTGCAACCGGCTACCTCCGCTC
AV2
401 GTCACGTGGGCGATCGACCTCAACGCCGGCGGCGCCGCGTTGCTGATCGCCTTGCTCATCGCTGCCGGGCAGCGGCTGCTTTATATTCCCGGGCGCACGG
CAGTGCACCCGCTAGCTGGAGTTGCGGCCGCCGCGGCGCAACGACTAGCGGAACGAGTAGCGACGGCCCGTCGCCGACGAAATATAAGGGCCCGCGTGCC
P91

RESULTS

Optimization

The initial focus of preliminary experiments was to detect MAC species/subspecies by choosing a set of oligonucleotide primers that would provide optimal product selectivity, sensitivity, and yield. Originally, a primer set named Av22a/Av22b was chosen that targeted a 91 bp fragment common to all MAC bacteria (kindly provided by F.A.K. El-Zaatari, Baylor College of Medicine). Many attempts were made to amplify this fragment in positive controls by conducting serial dilution trails that varied the concentrations of $MgCl_2$ and/or $MgSO_4$, DNA Taq polymerase, primers, and template. After exhausting all variables when using Av22a/Av22b PCR including these primers had poor success as Figure 4 illustrates. Consequently, more experiments were designed in order to determine why little progress was made in earlier optimization steps. This included re-evaluation of the selected primers with regard to several design criteria such as sequence content, nucleotide length, and melting and annealing temperatures. Surprisingly, it was discovered that the Av22a/Av22b primer set had a 10^{o}C difference between their melting and annealing temperatures. Normally, for primers to work optimally, their annealing temperatures need to be within ~2-4^{o}C of each other. Therefore, the next focus of the optimization process was to find primers for MAC that met standard design criteria, especially annealing temperature. Following an extensive literature search, several sets of primers were chosen that could detect and distinguish specific MAC subspecies. To continue

the optimization process, the 70 kDa heat shock protein (*hsp*x) characteristic of MAP was targeted. The MAP h-L/MAP h-R oligonucleotide primer set, which are 19 and 18 base pairs respectively, amplify a 211 bp fragment. Again, many experiments were designed that varied the PCR reagents and thermocycler conditions. Specifically, it was the concentration of oligonucleotide primers that had the greatest impact on hspx DNA amplification. When the primers, having an original concentration of 10uM, were diluted in a 1:50 solution of primer to TE buffer (10mM Tris, 0.1mM EDTA, pH 7.0), PCR specificity was greatly improved. Similarly, different Mg concentrations also influenced fragment amplification and became a critical factor in optimizing PCR specificity. High amounts of Mg favored primer-dimer formation and increased non-specific product yield, while low amounts decreased the level of desired product. For example, Figure 5 illustrates the results of the hspx PCR assay in which the concentrations of oligonucleotide primers and $MgCl_2$ were varied. Lane 15 contained 10 pmoles of undiluted primers and 0.1 umoles of $MgCl_2$ and shows a faint 211 bp DNA band indicating the presence of the hspx gene. Lanes 17 and 19 contained the same level of primers (10 pmoles) and increased amounts of $MgCl_2$ (0.3 umoles & 0.4 umoles, respectively) and show no detection of the hspx in positive control samples. These relatively high levels of primer and Mg produced large dimers which interfered with the detection of the 211 bp hspx fragment. On the other hand, lanes 9, 11, and 13 show clear positive results for the 211 bp hspx fragment, whereby the $MgCl_2$ level was at a constant 0.2 umoles amount and the primer quantities were 0.2 pmoles , 0.4 pmoles, and 0.8 pmoles, respectively. Consequently, lane 11 showed optimal amplification of the 211 bp hspx fragment with little dimer formation; this occurred when primer amounts were relatively low (0.4 pmoles) and $MgCl_2$ were high (0.4 umoles).

Figure 4. Early PCR Optimization Results using Av22a/Av22b oligonucleotide primers for the detection of MAC.

M corresponds to a 1 Kb 100 base pair DNA step ladder. (A) shows an agarose gel that corresponds to an experiment in which the PCR reaction contained 5 pmoles of each primer, 0.15 umoles of $MgCl_2$, 1.75 units of DNA Taq Polymerase Sequencing Grade and 5 uL of MAP template. The number of amplification cycles in the thermocycler were varied in 7 cycle intervals for lanes 1, 2, 3, 4 & 5. Lane 5 shows a faint 91 bp fragment indicating the presence of MAC DNA. (B) shows an agarose gel that corresponds to an experiment in which the PCR reaction contained 5 pmoles of each primer, 1.75 units of DNA Taq Polymerase Sequencing Grade, 5 uL of MAP template, and varying amounts of $MgCl_2$. Lanes 4 & 5 contained 0.1 umoles & 0.3 umoles of $MgCl_2$, respectively, and show faint 91 bp fragments indicating the presence of MAC DNA.

A

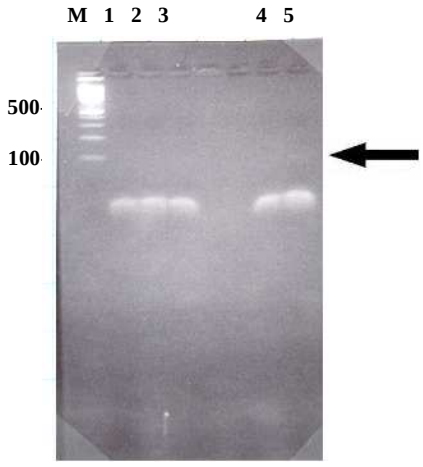

B

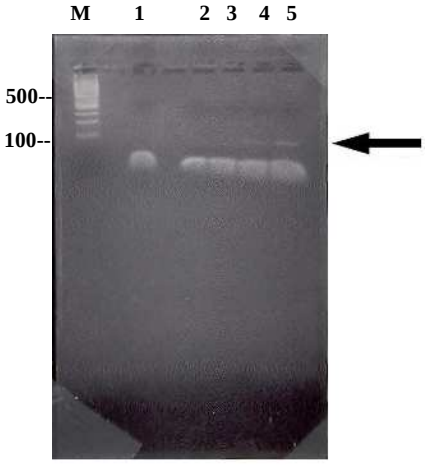

Figure 5. Optimization of $MgCl_2$ versus Oligonucleotide Primer Concentrations in Hspx PCR Assay.

M corresponds to a 1 Kb 100 bp DNA step ladder. Lanes 1 & 2 correspond to negative controls. Lanes 3 & 4 correspond to a PCR reaction containing 10 pmoles of each primer and 0.2 umoles $MgCl_2$. Lane 6 contains 0.2 pmoles of each primer and 0.2 umoles MgCl2. Lane 7 contains 0.4 pmoles of each primer and 0.2 umoles $MgCl_2$. Lane 8 contains 0.8 pmoles of each primer and 0.2 umoles $MgCl_2$. Lane 9 contains 10 pmoles of each primer and 0.1 umoles $MgCl_2$. Lane 10 contains 10 pmoles of each primer and 0.3 umoles $MgCl_2$. Lane 11 contains the same reagent concentrations as lanes 3 & 4, except it has 1.25 units of DNA Taq Polymerase instead of 5 units like all the other reactions. Lanes 6, 7, 8, & 9 show 211 bp DNA fragments indicative of the hspx specific to MAP.

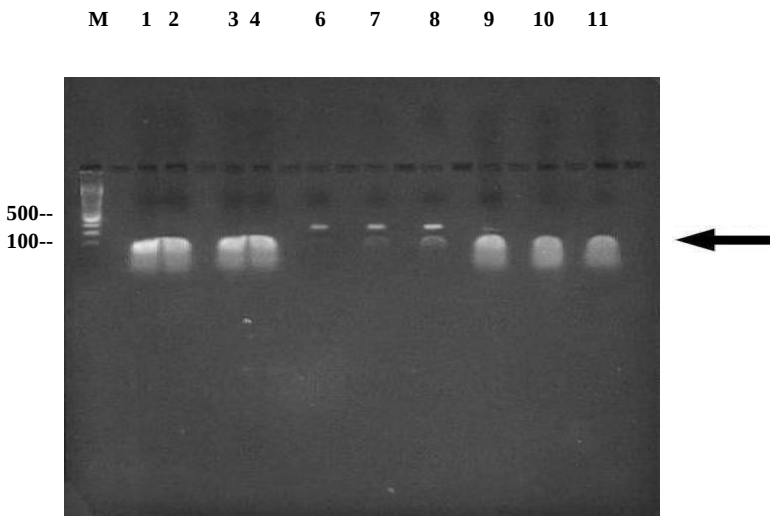
M 1 2 3 4 6 7 8 9 10 11
500--
100--

Several experiments were performed using different types of DNA Taq polymerase in order to determine which one would provide optimal sensitivity as well as allow for a time effective thermocycler protocol. Red Taq Polymerase (Sigma) was tried early in the optimization process with little success (no data shown). DNA Taq Polymerase Sequencing Grade did yield moderate sensitivity yet required extensive cycling conditions. Finally, Platinum Hi-Fidelity DNA Taq Polymerase (Invitrogen), as opposed to others tried, increased the clarity and intensity of DNA fragments while reducing the time needed for amplification. Figure 6 shows a comparison of DNA Taq Polymerase Sequencing Grade and Platinum Hi-Fidelity DNA Taq Polymerase and thermocycling protocols in which they worked best. The amount of template was also modified in order to allow for sensitivity of low DNA copy number without incurring detection interference. Extracted DNA concentrations varied considerably, consequently, a large amount of template (10 uL) was used in each PCR reaction. Knowing the high G+C content in mycobacteria, the DNA co-solvent betaine was explored as an alternative to DMSO to further optimize the sensitivity of the PCR assays by minimizing secondary structure formation, thereby enhancing primer annealing. Experimental results demonstrated that 25.5 umoles of betaine was the optimum amount required in the PCR reaction mixture to yield the greatest fragment amplification (Figure 8).

Throughout the optimization process, the thermocycler conditions were refined for optimal selectivity and sensitivity based upon the the calculated annealing temperatures of the primers as well as the length of the desired PCR product. Table 1 provides an overview of all relevant

information related to primer selections and optimization, particularly melting and annealing temperatures.

Table 1: Primer Selections for PCR Panel to Detect and Distinguish Members of MAC

MAC ss	ss. loci	PCR product	Primer name	Orientation and sequence	Tm (ºC)	Ta (ºC)
* M. Avium Complex	16S rRNA	193 bp	A-16-L	5'-AGAGTTTGATCCTGGCTCAG-3'	58	53
			A-16-R	5'-ACCAGAAGACATGCGTCTTG-3'	58	53
** M. Avium Complex	IS1245	427 bp	MAC-L	5'-GCCGCCGAAACGATCTAC-3'	58	53
			MAC-R	5'-AGGTGGCGTCGAGGAAGAC-3'	62	57
MA para-tuberculosis	IS900	401 bp	P90	5'-GTTCGGGGCCGTCGCTTAGG-3'	67	62
			P91	5'-GAGGTCGATCGCCCACGTGA-3'	65	60
MA para-tuberculosis	IS900	298 bp	AV1	5'-ATGTGGTTGCTGTGTTGGATGG-3'	62	57
			AV2	5'-CCGCCGCAATCAACTCCAG-3'	62	57
[A] MA para-tuberculosis	Hspx	211bp	Map h-L	5'-GACCGGCTATCTGTGGAAC-3'	60	55
			Map h-R	5'-CTCGTCGGCTTGCACCTG-3'	61	56
[B] ***M. Avium Complex	--	91 bp	Av22a	5'-CGCCGGAAAACGCCGTG-3'	60	55
			Av22b	5'-CGTAACACGAAGACGTA-3"	50	45

*M. Avium Complex includes MAV and MAP; ** M. Avium Complex includes MAV and MI (more typing necessary due to limited strain detection in MI); ***M. Avium Complex includes MAV, MI, and MAP

[A] Hspx Assay discontinued due to poor success in samples (low copy number)

[B] Assay discontinued due to poor success in samples (10ºC in annealing temperatures)

Figure 6. PCR Optimization of Different DNA Taq Polymerases versus Thermocycling Conditions in the Detection of MAP using P90/P91 primer set.

(A) shows an agarose gel that corresponds to an experiment in which DNA Taq Polymerase Sequencing Grade was used with thermocycling conditions as follows: an initial 5 minute hot start at 94°C and 39 cycles of: 1 minute denaturation at 94°C, 1 minute primer annealing at 58°C, and 3 minutes extension at 72°C. M corresponds to a 1 Kb 100 bp DNA step ladder. Lanes 1 & 2 show bands for the 401 bp fragment of IS900 after the first round of nested PCR using 10 uL of MAP template (Kay & Linda DNA, respectively). (B) shows an agarose gel that corresponds to an experiment in which Platinum Hi-Fidelity DNA Taq Polymerase and DNA Taq Polymerase Sequencing Grade were compared and used with thermocycler conditions as follows: an initial 5 minute hot start at 94°C and 30 cycles of: 45 second denaturation at 94°C, 30 primer annealing at 56°C, and 2 minutes extension at 72°C. M corresponds to a Low Density 100 base pair DNA step Ladder. Lane 1 contains DNA Taq Polymerase Sequencing Grade and shows no visible band, while Lane 2 contains the Platinum Hi-Fidelity DNA Taq Polymerase and shows a 401 bp fragment for the IS900 gene indicating MAP (4 uL load onto gel). Lanes 3 & 4 show the same samples respectively (20 uL load onto gel).

A

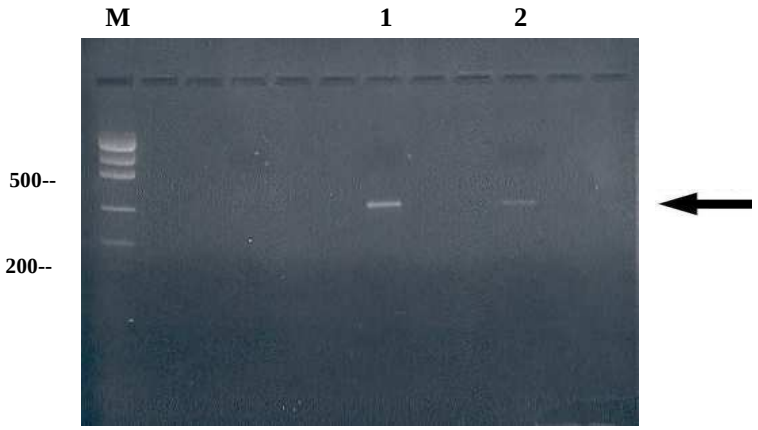

B

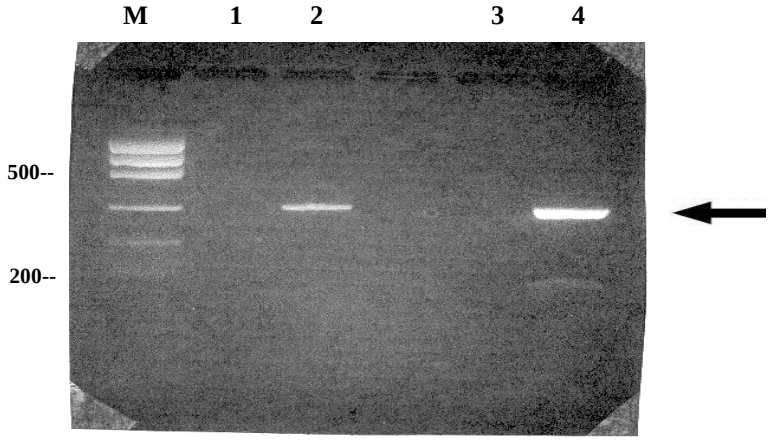

Additionally, the optimal PCR reaction cocktail mixture was identified which encompassed a common PCR reaction mixture that positively amplified all previously mentioned DNA fragments that indicate the presence of *Mycobacterium avium* subspecies. The optimal PCR reaction included 17 uL of sterile H2O, 5 uL of 10x Hi-Fi buffer (Invitrogen), 8.5 uL of 3 M betaine, 1 uL of 10 mM dNTP's (Fisher Scientific), 4 uL of 50 mM MgSO4 (Invitrogen), 2 uL each of 10 mM specific oligonucleotide primer, and 0.5 uL of 100 unit Platinum Hi-Fi Taq polymerase (Invitrogen). The total volume of the PCR reaction was brought to 50 uL by the addition of 10 uL of template DNA from each extracted sample. The individual PCR reactions were then placed into a thermocycler (Biorad) with programmed conditions that allowed the amplification of all mentioned DNA fragments depending upon on the added primers.

The program began with a 5 minute hot start to ensure full DNA denaturation followed by 30 cycles of the following steps: denaturation at 94^{o} C for 45 seconds, primer annealing at 56^{o} C for 30 seconds, and extension at 72^{o} C for 2 minutes. The thermocycler protocol ended with a final 72^{o} C extension for 10 minutes followed by a 4^{o} C indefinite hold. Figures 7I and 7II illustrate the progression of PCR conditions within the thermocycler as well as the final concentration of specific reagents used in the PCR reaction before and after the final optimization. Finally, Figure 8 shows a comparison of the early optimization versus final optimization results for all three PCR assays used in this study.

Once a practical protocol for optimal amplification of desired products was developed, it was applied to DNA samples obtained from the gut tissue of 100 test subjects. Specifically, these

three PCR assays used in this investigation were performed on all DNA obtained from cultured mycobacterial isolates.

Figure 7-I. Thermocycler Protocols and PCR Reagent Concentrations after Optimization.

(A) shows the final thermocycler conditions upon optimization completion.
(B) shows the final PCR reagent concentrations.

A

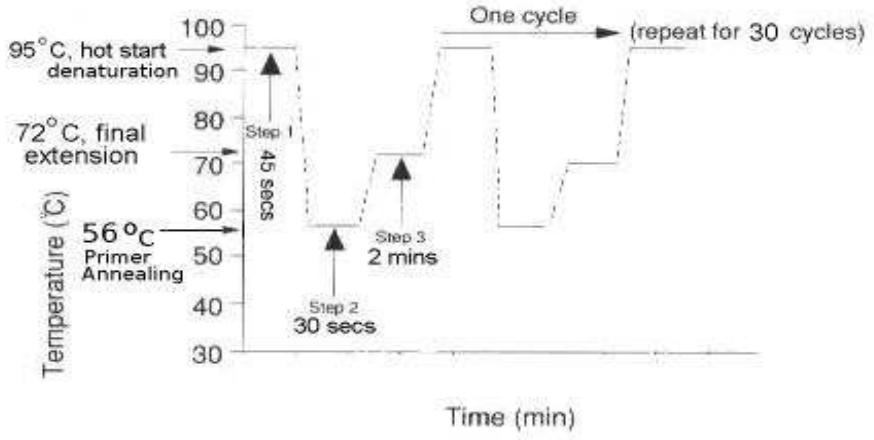

B

Sterile H20	17 uL
10x Hi-Fi Buffer	5 uL
3 M Betaine	8.5 uL
10 mM dNTP Mix	1 uL
50 mM MgSO4	4 uL
10 uM Primer (1:50 dilution)	2 uL (each)
100 u Platinum Hi-Fi DNA Taq Polymerase	0.5 uL
Template DNA	10 uL
Total Volume	50 uL

Figure 7-II. Thermocycler Protocols and PCR Reagent Concentrations before Optimization.

(A) shows the preliminary thermocycler conditions before optimization completion.
(B) shows the preliminary PCR reagent concentrations.

A

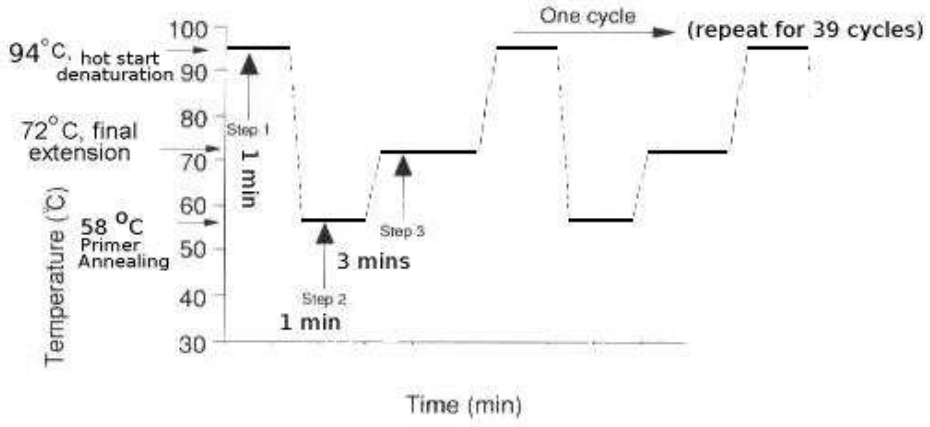

B

Sterile H20	31.75 uL
10x Buffer w/ $MgCl_2$	5 uL
DMSO	5 uL
10 uM Primer (1:50 dilution)	1 uL (each)
10 mM dNTP Mix	1 uL
100 u DNA Taq Polymerase Sequencing Grade	0.25 uL
Template DNA	5 uL
Total Volume	50 uL

Figure 8. Comparison of Early Optimization Trials versus Final Optimization Trials for all PCR Assays used in this Study.

(A) shows a primer test using DNA Taq Polymerase Sequencing Grade used with thermocycler conditions before optimization (use of DMSO). M corresponds to a 1Kb 100 bp DNA step ladder. Lane 1=negative control (IS900; MAP), Lane 2=negative control (Hspx; MAP), Lane 3=negative control (IS1245; MAV), Lane 4=negative control (16 S rRNA; MAV), Lane 5=positive control (IS900; MAP; no visible 401 bp fragment), Lane 6=positive control (Hspx; MAP; 211 bp), Lane 7=positive control (IS1245; MAV; no visible 427 bp fragment), Lane 8=positive control (16 S rRNA; MAP; 193 bp), Lane 9=positive control (16 S rRNA;MAV; 193 bp). (B) shows a primer test using Platinum Hi-Fidelity DNA Taq Polymerase with thermocycler conditions after optimization (use of betaine). M corresponds to a 1Kb 100 bp DNA step ladder. Lane=negative control (IS1245), Lane 2=positive control (IS1245; MAV; 427 bp), Lane 3=negative control (16 S rRNA), Lane 4=positive control (16 S rRNA; MAV; 193 bp), Lane 5=negative control (16 S rRNA), Lane 6=positive control (16 S rRNA; MAP; 193 bp), Lane 7=negative control (Hspx), Lane 8=positive control (Hspx; MAP; 211 bp), Lane 9=negative control (IS900; 1st amplification), Lane 10=positive control (IS900; MAP; 401 bp; 1st amplification), Lane 11=negative control (IS900; 2nd amplification), Lane 12=positive control (IS900; MAP; 298 bp, 2nd amplification)

A

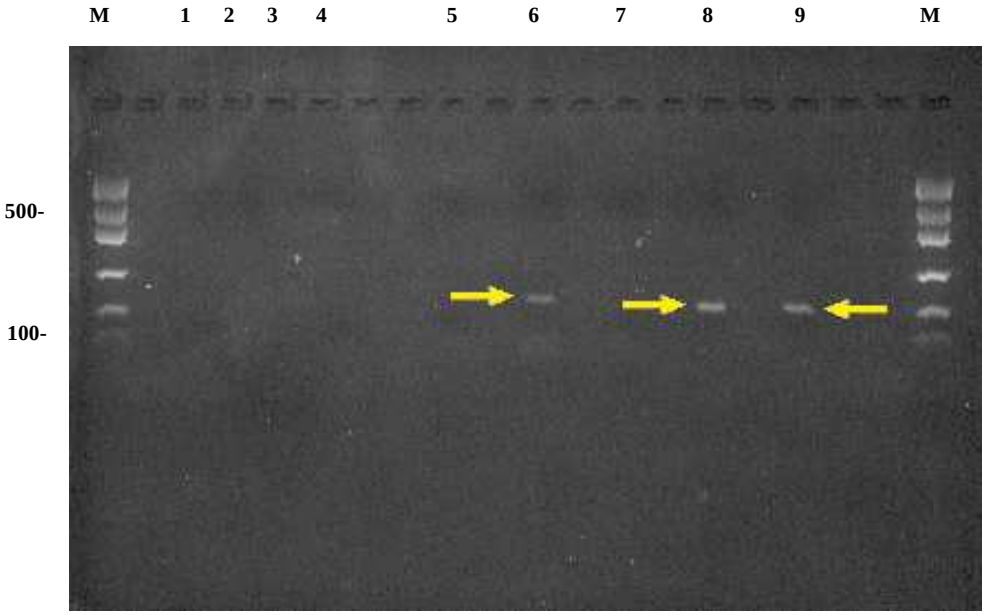

B

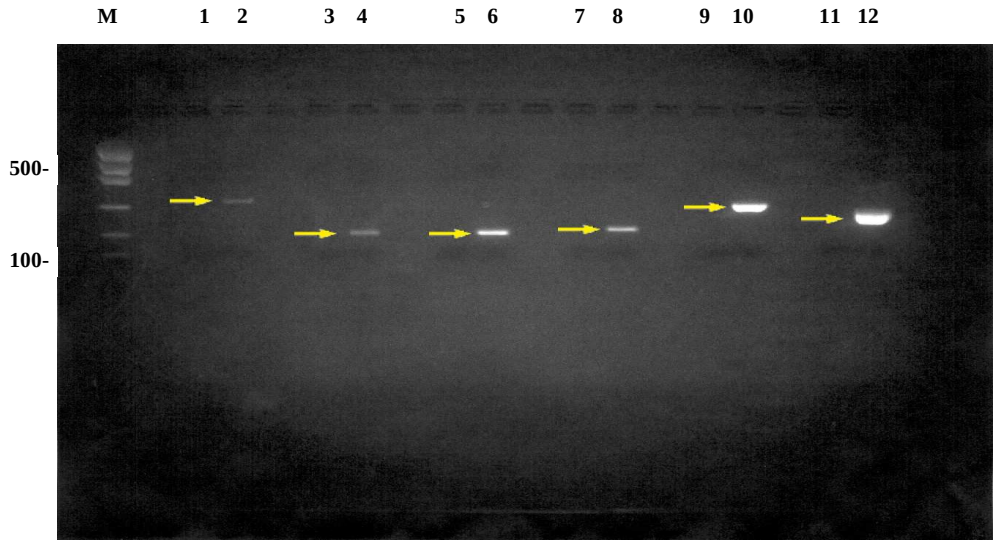

Specimen Processing

A total of 100 resected, full-thickness tissue samples removed from IBD patients were received from Mt. Sinai Hospital and included in this two year etiological study. Table 2 details the code as well as dates of collection and processing.

Table 2: Tissue Processing and Growth Time in Bactec Media

[A]Code	Collection Date	Process Date	Maximum GI Date	[B]Duration
MS8	11/07/01	11/08/01	12/03/01	25
MS8e	11/07/01	11/08/01	12/03/01	25
MS11	11/08/01	11/09/01	12/03/01	24
MS11e	11/08/01	11/09/01	12/03/01	24
MS12	11/14/01	11/15/01	12/03/01	18
MS12e	11/14/01	11/15/01	12/03/01	18
MS13e	11/14/01	11/15/01	12/03/01	18
MS19e	11/16/01	11/17/01	12/03/01	16
MS21	11/20/01	11/21/01	12/03/01	12
MS21e	11/20/01	11/21/01	12/07/01	16
MS22	11/20/01	11/21/01	12/07/01	16
MS22e	11/20/01	11/21/01	12/07/01	16
MS24e	11/20/01	11/21/01	12/07/01	16
MS25	11/27/01	11/28/01	12/26/01	28
MS25e	11/27/01	11/28/01	12/11/01	13
MS29	11/29/01	11/30/01	12/11/01	11
MS30	11/29/01	11/30/01	12/11/01	11
MS32	12/04/01	12/05/01	12/26/01	21
MS41e	12/14/01	12/15/01	01/02/02	18
MS47	01/09/02	01/10/02	01/22/02	12
MS62e	01/30/02	01/31/02	02/25/02	25
MS67	02/04/02	02/05/02	02/25/02	20
MS68	02/04/02	02/05/02	02/25/02	20
MS71	02/05/02	02/06/02	02/25/02	19
MS71e	02/05/02	02/06/02	03/11/02	34
MS83	02/12/02	02/13/02	03/11/02	27
MS92	03/04/02	03/05/02	04/09/02	35
MS92e	03/04/02	03/05/02	04/09/02	35

[A] Refers to codes blindly assigned to tissue samples; [B] Refers to duration of bacterial growth in days

Once prepared, the individual tissue specimens were inoculated into the Bactec and MGIT culture systems. Two Bactec media bottles were used for each sample and contained nutrients and supplements previously described; one of the bottles included the addition of egg yolk. Consequently, a total of 200 Bactec samples were used for this project. Accordingly, one MGIT culture tube was inoculated from each processed tissue, for a total of 100 MGIT culture specimens. Tables 3, 4, and 5 outline the type of media used for each sample.

Table 3: Documentation of Received IBD Tissues and Media Types Used for Samples 1-37

[A]Code	Collection Date	Date Received	Media Type		
			B+E	B-E	MGIT
1	10/25/01	10/26/01	✔	✔	✔
2	10/26/01	10/27/01	✔	✔	✔
3	10/30/01	10/31/01	✔	✔	✔
4	10/31/01	11/01/01	✔	✔	✔
5	10/31/01	11/01/01	✔	✔	✔
6	10/31/01	11/01/01	✔	✔	✔
7	11/01/01	11/02/01	✔	✔	✔
8	11/07/01	11/08/01	✔	✔	✔
9	11/08/01	11/09/01	✔	✔	✔
10	11/08/01	11/09/01	✔	✔	✔
11	11/08/01	11/09/01	✔	✔	✔
12	11/14/01	11/15/01	✔	✔	✔
13	11/14/01	11/15/01	✔	✔	✔
14	11/14/01	11/15/01	✔	✔	✔
15	11/15/01	11/16/01	✔	✔	✔
16	11/16/01	11/17/01	✔	✔	✔
17	11/16/01	11/17/01	✔	✔	✔
18	11/16/01	11/17/01	✔	✔	✔
19	11/16/01	11/17/01	✔	✔	✔
20	11/20/01	11/21/01	✔	✔	✔
21	11/20/01	11/21/01	✔	✔	✔
22	11/20/01	11/21/01	✔	✔	✔
23	11/20/01	11/21/01	✔	✔	✔
24	11/20/01	11/21/01	✔	✔	✔
25	11/27/01	11/28/01	✔	✔	✔
26	11/28/01	11/29/01	✔	✔	✔
27	11/28/01	11/29/01	✔	✔	✔
28	11/29/01	11/30/01	✔	✔	✔
29	11/29/01	11/30/01	✔	✔	✔
30	11/29/01	11/30/01	✔	✔	✔
31	12/03/01	12/04/01	✔	✔	✔
32	12/04/01	12/05/01	✔	✔	✔
33	12/05/01	12/06/01	✔	✔	✔
34	12/06/01	12/07/01	✔	✔	✔
35	12/06/01	12/07/01	✔	✔	✔
36	12/06/01	12/07/01	✔	✔	✔
37	12/10/01	12/11/01	✔	✔	✔

Table 4: Documentation of Received IBD Tissues and Media Types Used for Samples 38-74

[A]Code	Collection Date	Date Received	Media Type		
			B+E	B-E	MGIT
38	12/10/01	12/11/01	✔	✔	✔
39	12/11/01	12/12/01	✔	✔	✔
40	12/11/01	12/12/01	✔	✔	✔
41	12/14/01	12/15/01	✔	✔	✔
42	12/14/01	12/15/01	✔	✔	✔
43	12/14/01	12/15/01	✔	✔	✔
44	01/08/02	01/09/02	✔	✔	✔
45	01/08/02	01/09/02	✔	✔	✔
46	01/09/02	01/10/02	✔	✔	✔
47	01/09/02	01/10/02	✔	✔	✔
48	01/09/02	01/10/02	✔	✔	✔
49	01/10/02	01/11/02	✔	✔	✔
50	01/10/02	01/11/02	✔	✔	✔
51	01/15/02	01/16/02	✔	✔	✔
52	01/15/02	01/16/02	✔	✔	✔
53	01/15/02	01/16/02	✔	✔	✔
54	01/17/02	01/18/02	✔	✔	✔
55	01/17/02	01/18/02	✔	✔	✔
56	01/17/02	01/18/02	✔	✔	✔
57	01/22/02	01/23/02	✔	✔	✔
58	01/23/02	01/24/02	✔	✔	✔
59	01/28/02	01/29/02	✔	✔	✔
60	01/29/02	01/30/02	✔	✔	✔
61	01/29/02	01/30/02	✔	✔	✔
62	01/30/02	01/31/02	✔	✔	✔
63	01/30/02	01/31/02	✔	✔	✔
64	01/31/02	02/01/02	✔	✔	✔
65	02/04/02	02/05/02	✔	✔	✔
66	02/04/02	02/05/02	✔	✔	✔
67	02/04/02	02/05/02	✔	✔	✔
68	02/04/02	02/05/02	✔	✔	✔
69	02/05/02	02/06/02	✔	✔	✔
70	02/05/02	02/06/02	✔	✔	✔
71	02/05/02	02/06/02	✔	✔	✔
72	02/05/02	02/06/02	✔	✔	✔
73	02/07/02	02/08/02	✔	✔	✔
74	02/07/02	02/08/02	✔	✔	✔

Table 5: Documentation of Received IBD Tissues and Media Types Used for Samples 75-100

[A]Code	Collection Date	Date Received	Media Type		
			B+E	B-E	MGIT
75	02/07/02	02/08/02	✔	✔	✔
76	02/07/02	02/08/02	✔	✔	✔
77	02/07/02	02/08/02	✔	✔	✔
78	02/07/02	02/08/02	✔	✔	✔
79	02/07/02	02/08/02	✔	✔	✔
80	02/11/02	02/12/02	✔	✔	✔
81	02/11/02	02/12/02	✔	✔	✔
82	02/12/02	02/13/02	✔	✔	✔
83	02/12/02	02/13/02	✔	✔	✔
84	02/14/02	02/15/02	✔	✔	✔
85	02/14/02	02/15/02	✔	✔	✔
86	02/19/02	02/20/02	✔	✔	✔
87	02/19/02	02/20/02	✔	✔	✔
88	02/19/02	02/20/02	✔	✔	✔
89	02/20/02	02/21/02	✔	✔	✔
90	02/20/02	02/21/02	✔	✔	✔
91	02/27/02	02/28/02	✔	✔	✔
92	03/04/02	03/05/02	✔	✔	✔
93	03/04/02	03/05/02	✔	✔	✔
94	03/05/02	03/06/02	✔	✔	✔
95	03/05/02	03/06/02	✔	✔	✔
96	03/19/02	03/20/02	✔	✔	✔
97	03/19/02	03/20/02	✔	✔	✔
98	03/21/02	03/22/02	✔	✔	✔
99	03/21/02	03/22/02	✔	✔	✔
100	04/11/02	04/12/02	✔	✔	✔
Total Cultures			100	100	100
Total Bactec Cultures			200		

[A] Refers to codes blindly assigned to tissue samples (Table 3-5)

Mycobacterial Growth in Bactec Media

All Bactec bottles were evaluated for bacterial growth using the Bactec 460 TB system. Of the 200 Bactec cultures, 13 bottles containing egg yolk and 15 bottles without egg yolk reached a

maximum growth index of 999. In all, a total of 28 cultures, comprised of tissue samples from 20 IBD subjects, produced bacterial growth using the Bactec media system. Eight of those individual tissue specimens exhibited bacterial growth in both types of Bactec culture media (+ egg yolk and – egg yolk supplement). Ranging from 11 to 34 days of incubation at 37° C with 5% CO_2, the 28 positive specimens took an average of 20.5 days to obtain a maximum growth reading. Table 2 (listed above) summarizes the list of samples that showed growth using the Bactec system as well as the amount of time required to reach a GI of 999. All Bactec bottles with suspected mycobacteria growth were removed from the incubator and subjected to further investigation as follows: A volume of 0.5 mL of culture was aseptically transferred into a 1.5 mL eppendorf tube for genomic DNA extraction and subsequent PCR analysis. An additional 50 uL aliquot of culture was used for Ziehl-Neelsen acid-fast staining. Table 6 illustrates the acid-fast status of each Bactec culture and/or subculture that demonstrated growth. All 28 samples that gave a 999 reading were then evaluated by PCR assay using primers specific for the 16S rRNA internal spacer region. This 193 bp DNA fragment, indicative of M. avium complex (MAC), was detected in 26/28 (93%) of suspect Bactec cultures. Table 1 (listed above) references the specific MAC loci, expected PCR product size, and primer sequences for all PCR assays used in this study.

Table 6: Acid-fast Results on Bactec Cultures and Subcultures

Tissue Sample Code	Acid-fast
MS8	+
MS8e	+
MS11	+
MS11e	+
MS12	+
MS12e	+
MS13e	+
MS19e	+
MS21	+
MS21e	+
MS22	+
MS22e	+
MS24e	+
MS25	+
MS25e	+
MS29	+
MS30	+
MS32	+
MS41e	-*
MS47	+*
MS62e	+*
MS67	-*
MS68	+*
MS71	-*
MS71e	+*
MS83	+*
MS92	+*
MS92e	+*

+: was determined to be positive in both cultures and subcultures
*: staining was done only on subcultures.

A representative set of these 16S rRNA results is shown in Figure 9.Only sample MS71 did not exhibit the presence of the 193 bp PCR product, indicating the absence of MAC DNA. However, unlike sample 71, acid-fast revealed that culture 71e contained acid-fast bacteria. Table 7 categorizes samples contain MAC DNA based on the results of the 16S rRNA.

Table 7: Results of the 16S rRNA PCR Assay on Positive Bactec Cultures

[A]Code	[B]Duration	16S rRNA PCR result	Conclusion
MS8	25	+	MAC
MS8e	25	+	MAC
MS11	24	+	MAC
MS11e	24	+	MAC
MS12	18	+	MAC
MS12e	18	+	MAC
MS13e	18	+	MAC
MS19e	16	+	MAC
MS21	12	+	MAC
MS21e	16	+	MAC
MS22	16	+	MAC
MS22e	16	+	MAC
MS24e	16	+	MAC
MS25	28	+	MAC
MS25e	13	+	MAC
MS29	11	+	MAC
MS30	11	+	MAC
MS32	21	+	MAC
MS41e	18	+	MAC
MS47	12	+	MAC
MS62e	25	+	MAC
MS67	20	+	MAC
MS68	20	+	MAC
MS71	19	-	Other than MAC
MS71e	34	-	Other than MAC
MS83	27	+	MAC
MS92	35	+	MAC
MS92e	35	+	MAC

[A] Refers to codes blindly assigned to tissue samples; [B] Refers to duration of bacterial growth in days

Figure 9. 16 S rRNA PCR Assay Results for Representative Set of Bactec Cultures.

M corresponds to a 1Kb 100 bp DNA step ladder. Lanes 1 & 2=negative controls. Lane 3=MS8, Lane 4=MS8e, Lane 5=MS11e, Lane 6=12, Lane 7=MS12e, Lane 8=MS13e, Lane 9=19e, Lane 10=MS21, Lane 11=MS21e, Lane 12=MS22, Lane 13=MS22e, Lane 14=MS62e, Lane 15=MS67, Lane 16=MS68, Lane 17=MS71, Lane 18=positive control (MAV; 193 bp)

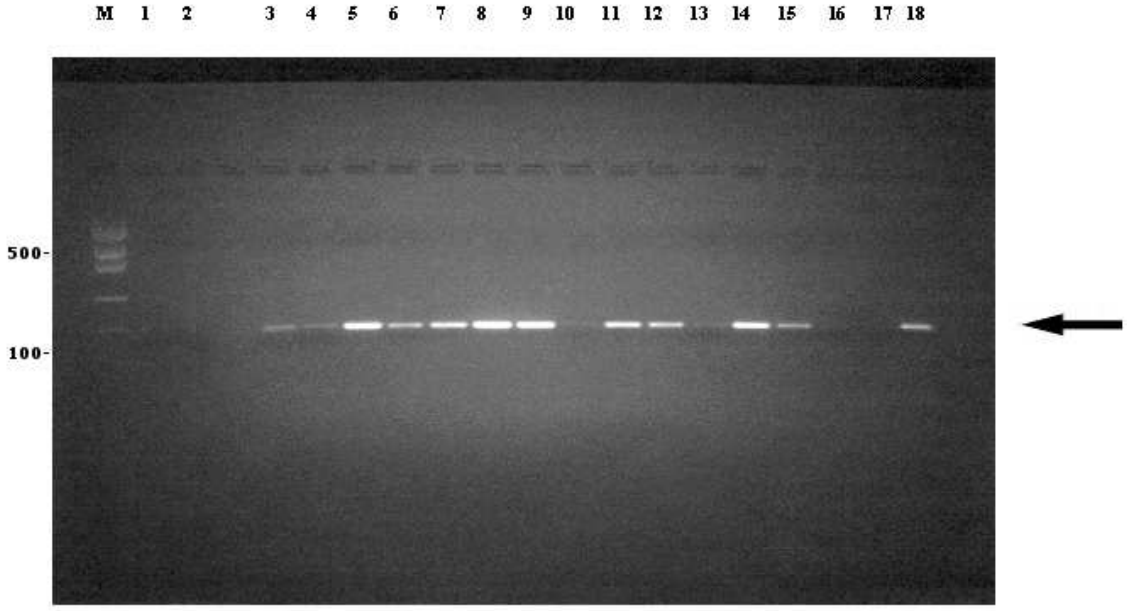
M 1 2 3 4 5 6 7 8 9 10 11 12 13 14 15 16 17 18
500-
100-

Therefore, these results demonstrate the presence of MAC in 93% of harvested Bactec bottles. In order to identify the particular member of the MAC present in the positive Bactec cultures, further PCR analysis using IS1245 specific primers indicative of M. avium avium (MAV) was performed. The assay revealed that 25 Bactec tissue cultures (89%) tested positive for the 427 bp IS1245 DNA fragment. Figure 10 shows a representative set of these IS1245 assay results. Additionally, Table 8 shows the results of the IS1245 PCR assay. An additional nested PCR assay was conducted to further determine the presence of M. avium paratuberculosis (MAP). The first part of the assay detected a 401 bp portion of the IS900 insertional element not normally visible after electrophoresis analysis because of low copy number. In order for the IS900 fragment to be seen, the PCR product from the first assay was used as a template for the second round of amplification. Consequently, the resulting 298 bp fragment of the IS900 DNA amplicon was only seen after a second round of PCR. A total of 6 Bactec cultures (21%) showed a positive result for the IS900 DNA sequence indicative of MAP. Figure 11 illustrates a representative set of the IS900 nested PCR results on Bactec cultures. Table 9 summarizes the results of nested PCR on all positive Bactec bottles.

Figure 10. IS1245 PCR Assay Results for Representative Set of Bactec Cultures.

M corresponds to a 1Kb 100 bp DNA step ladder. Lanes 1 & 2=negative controls. Lane 3=MS8, Lane 4=MS8e, Lane 5=MS11, Lane 6=MS11e, Lane 7=MS12, Lane 8=MS12e, Lane 9=MS13e, Lane 10=MS19e, Lane 11=MS21, Lane 12=MS21e, Lane 13=MS22, Lane 14=MS22e, Lane 15=MS24e, Lane 16=MS25, Lane 17=MS25e. Lane 18=positive control (MAV; 427 bp). Lane 19 shows no band and corresponds to positive control MAP DNA.

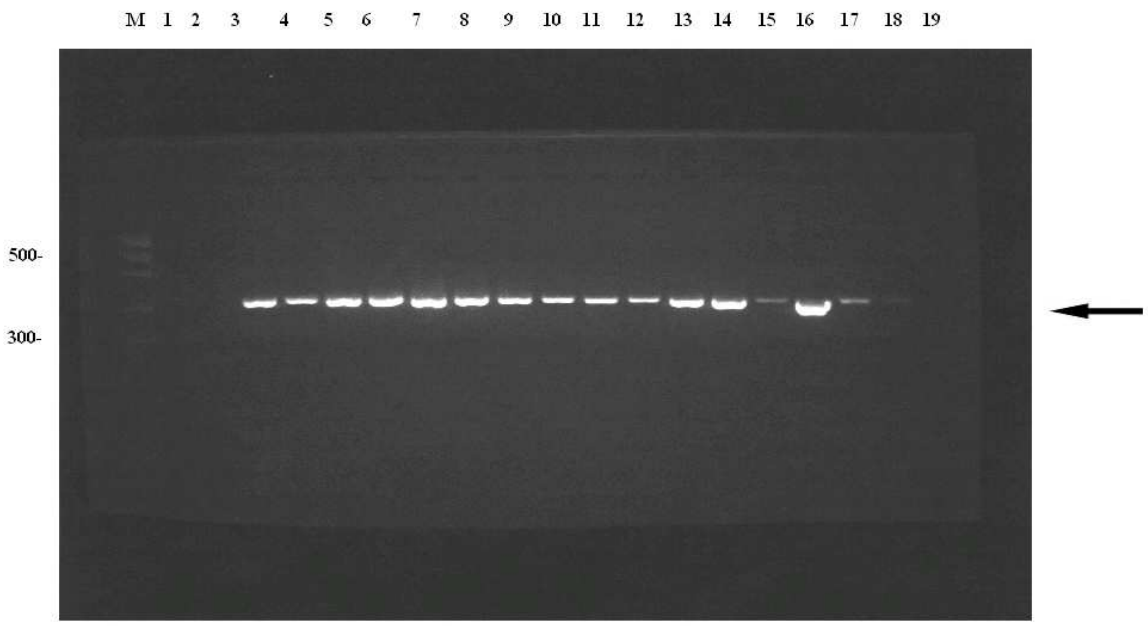
M 1 2 3 4 5 6 7 8 9 10 11 12 13 14 15 16 17 18 19
500-
300-

Table 8: Results of the IS1245 PCR Assay on Positive Bactec Cultures

[A]Code	[B]Duration	IS1245 PCR result	Conclusion
MS8	25	+	MAV
MS8e	25	+	MAV
MS11	24	+	MAV
MS11e	24	+	MAV
MS12	18	+	MAV
MS12e	18	+	MAV
MS13e	18	+	MAV
MS19e	16	+	MAV
MS21	12	+	MAV
MS21e	16	+	MAV
MS22	16	+	MAV
MS22e	16	+	MAV
MS24e	16	+	MAV
MS25	28	+	MAV
MS25e	13	+	MAV
MS29	11	-	MAC
MS30	11	+	MAV
MS32	21	+	MAV
MS41e	18	+	MAV
MS47	12	+	MAV
MS62e	25	+	MAV
MS67	20	+	MAV
MS68	20	+	MAV
MS71	19	-	Other than MAC*
MS71e	34	-	Other than MAC*
MS83	27	+	MAC
MS92	35	+	MAC
MS92e	35	+	MAC

[A] Refers to codes blindly assigned to tissue samples

[B] Refers to duration of bacterial growth in days

*Other than MAC conclusion based upon acid-fast staining morphology

Table 9: Results of the IS900 Nested PCR Assay on Positive Bactec Cultures

[A]Code	[B]Duration	IS900 nested PCR	Conclusion
MS8	25	-	MAV
MS8e	25	-	MAV
MS11	24	+	MAP
MS11e	24	+	MAP
MS12	18	-	MAV
MS12e	18	-	MAV
MS13e	18	-	MAV
MS19e	16	-	MAV
MS21	12	-	MAV
MS21e	16	-	MAV
MS22	16	-	MAV
MS22e	16	-	MAV
MS24e	16	-	MAV
MS25	28	-	MAV
MS25e	13	-	MAV
MS29	11	-	MAC
MS30	11	+	MAP
MS32	21	-	MAV
MS41e	18	-	MAV
MS47	12	-	MAV
MS62e	25	-	MAV
MS67	20	-	MAV
MS68	20	-	MAV
MS71	19	-	Other than MAC
MS71e	34	+	Other than MAC
MS83	27	-	MAV
MS92	35	-	MAV
MS92e	35	+	MAP

[A] Refers to codes blindly assigned to tissue samples

[B] Refers to duration of bacterial growth in days

Figure 11. IS900 Nested PCR Assay Results for Representative Set of Bactec Cultures.

(A) corresponds to the 1st round of nested PCR using primers P90/P91. (B) corresponds to the 2nd round of nested PCR using primers Av1/Av2. M1 corresponds to a 1Kb 100 bp DNA step ladder. M2 corresponds to a 25 bp DNA step ladder. Lane 1=positive control {MAP; 401 bp (A); 298 bp (B), Lane 2=negative control, Lane 3=MS11e, Lane 4=MS11, Lane 5=MS22e, Lane 6=MS30, Lane 7=MS71e. The image of positive samples are from different agarose gels visualized at different times.

A

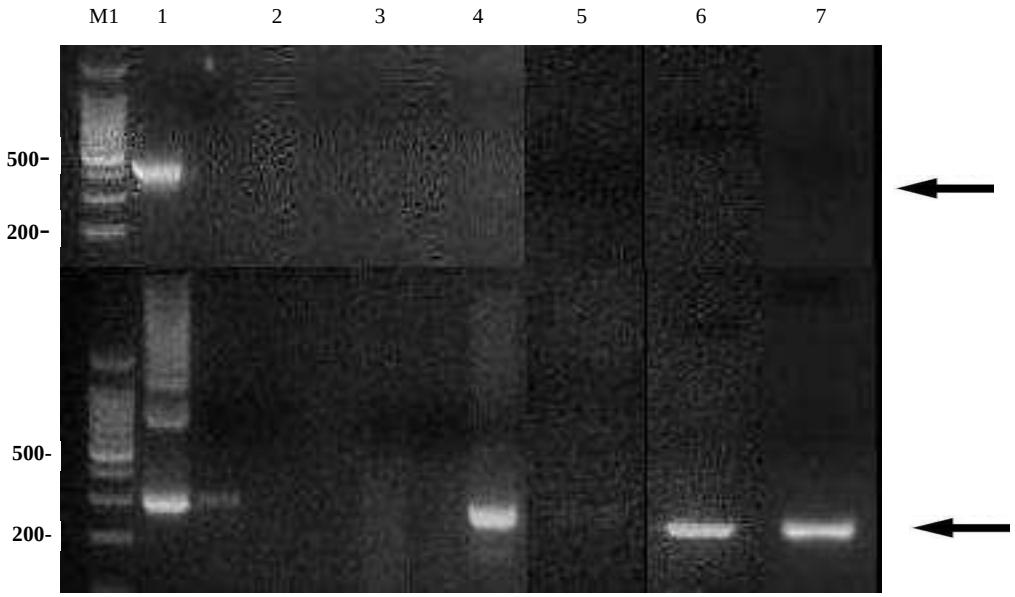

B

Overall, out of the 6 Bactec cultures confirmed to contain MAP, 5 (83%) showed positive results for all three assays: 16S rRNA, IS1245, and IS900 nested PCR. Table 10 concludes the MAC subspecies present in all 28 Bactec cultures based upon the overall PCR analysis.

Table 10: Summary of Three Assays on Bactec Cultures

[A]Code	[B]Duration	16S rRNA PCR Result	IS1245 PCR Result	IS900 Nested PCR Result	Conclusion
MS8	25	+	+	-	MAV
MS8e	25	+	+	-	MAV
MS11	24	+	+	-	MAV
MS11e	24	+	+	+	MAP
MS12	18	+	+	+	MAP
MS12e	18	+	+	-	MAV
MS13e	18	+	+	-	MAV
MS19e	16	+	+	-	MAV
MS21	12	+	+	-	MAV
MS21e	16	+	+	-	MAV
MS22	16	+	+	-	MAV
MS22e	16	+	+	+	MAP
MS24e	16	+	+	-	MAV
MS25	28	+	+	-	MAV
MS25e	13	+	+	-	MAV
MS29	11	+	-	-	MAC
MS30	11	+	+	+	MAP
MS32	21	+	+	-	MAV
MS41e	18	+	+	-	MAV
MS47	12	+	+	-	MAV
MS62e	25	+	+	-	MAV
MS67	20	+	+	-	MAV
MS68	20	+	+	-	MAV
MS71	19	-	-	-	Other than MAC
MS71e	34	-	-	+	Other than MAC
MS83	27	+	+	-	MAV
MS92	35	+	+	-	MAV
MS92e	35	+	+	+	MAP

[A] Refers to codes blindly assigned to tissue samples

[B] Refers to duration of bacterial growth in days

Furthermore, all suspect Bactec isolates were analyzed using multiplex PCR and IS900 DNA fingerprinting by a collaborator at The Ohio State University. Table 11 shows the IS900 copy number detected in each sample.

Table 11: IS900 DNA Copy Number in Samples that Tested IS900 Positive after Nested PCR

Sample Code	Media Type	UCF IS900 Result	Ohio IS900 Copy #
MS6	MGIT	-	0
MS8	Bactec	-	1
MS8e	Bactec	-	4
MS11	Bactec	+	1
MS11e	Bactec	+	4
MS12	Bactec	-	3
MS12e	Bactec	-	0
MS13e	Bactec	-	3
MS19e	Bactec	-	0
MS21	Bactec	-	0
MS21e	Bactec	-	3
MS22	Bactec	-	1
MS22e	Bactec	+	3
MS24e	Bactec	-	2
MS25	Bactec	-	3
MS25e	Bactec	-	1
MS29	MGIT	+	1
MS29	Bactec	-	nd
MS30	Bactec	+	1
MS32	Bactec	-	1
MS41e	Bactec	-	3
MS43	MGIT	+	nd
MS47	Bactec	-	0
MS62e	Bactec	-	1
MS67	Bactec	-	0
MS68	Bactec	-	nd
MS71	Bactec	-	nd
MS71e	Bactec	+	nd
MS83	Bactec	-	1
MS92	Bactec	-	0
MS92e	Bactec	+	1

nd: not determined

Subculture of Mycobacteria Grown in Bactec Media

All tissue samples cultured with the Bactec media system that achieved a growth index of 999 were subcultured using Mycobactosel L-J Medium slants enriched with Mycobactin J. Approximately 6-8 weeks of incubation at room temperature was necessary in order to observe visible colonies on the L-J media. Following acid-fast staining on all slant colonies, microscopic analysis revealed that 27/28 subculture samples (96%) contained acid-fast positive bacteria. Slant MS71e, which was confirmed as a non-MAC isolate, contains spiral-shaped, long acid-fast bacilli, compared to normal MAC isolates where short rod-shaped bacilli arranged in clumps were observed, as seen in Figure 12. Genomic DNA extraction was performed on all 28 subcultured isolates, and the DNA extracts were analyzed by a panel of PCR assays as previously described. After PCR evaluation using 16S rRNA primers, 23/28 samples (82%) proved to contain the 193 bp fragment of the internal spacer region (MAC). Twenty-four of the 28 samples (86%) gave positive results for the 427 bp IS1245 DNA array (MAV), while one sample (4%) indicated the presence of the 298 bp IS900 DNA sequence (MAP). Figure 13 shows the results from all three PCR assays on a representative set of Bactec subcultures. Table 12 summarizes all the PCR results conducted on the Bactec subcultures, and itemizes each type of organism detected.

Figure 12. Comparison of MAC Atypical versus Typical Acid-fast Bacilli Obtained from Bactec Subcultures.

(A) illustrates sample MS71e which contains spiral-shaped, acid-fast bacilli atypical of MAC. (B) depicts normal MAC isolates which contains short, rod-shaped acid-fast bacilli typical of MAC.

A

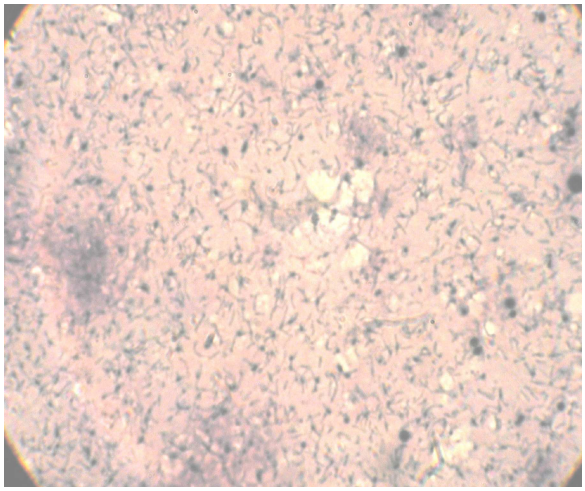

Unknown Acid-fast +

B

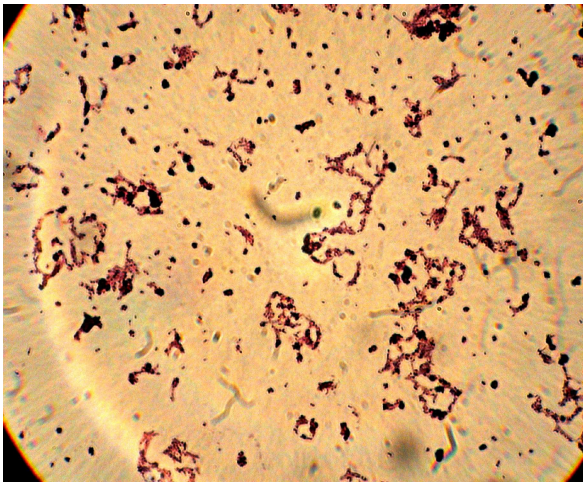

MAC Acid-fast +

Figure 13. Complete PCR Results for a Representative Set of Bactec Subcultures.

(A) represents the 16 S rRNA Assay. (B) represents the IS1245 Assay. (C) represents the IS900 nested PCR Assay. M corresponds to a 1 Kb 100 base pair DNA step ladder. (A) Lanes 1 & 2=negative controls, Lane 3=MS5A, Lane 4=MS5B, Lane 5=MS8, Lane 6=MS8e, Lane 7=MS10, Lane 8=MS11, Lane 9=MS11e, Lane 10=MS12, Lane 11=MS47, Lane 12=MS67, Lane 13=MS92e, Lane 14=positive control (MAV; 193 bp), Lane 15=positive control (MAP; 193 bp). (B) Lanes 1 & 2=negative controls, Lane 3=MS5A, Lane 4=MS5B, Lane 5=MS8, Lane 6=MS8e, Lane 7=MS10, Lane 8=MS11, Lane 9=MS11e, Lane 10=MS12, Lane 11=MS47, Lane 12=MS67, Lane 13=MS92e, Lane 14=positive control (MAV; 427 bp). (C) Lane 1, 2, 3=negative controls (Lane 1 is empty in P90/P91 gel), Lane 4=MS5A, Lane 5=MS5B, Lane 6=MS8, Lane 7=MS8e, Lane 8=MS10, Lane 9=MS11, Lane 10=MS11e, Lane 11=MS12, Lane 12=MS47, Lane 13=MS67, Lane 14=MS92e, Lane 15 & 16=positive control {MAP; 401 bp (P90/P91); 298 bp (Av1/Av2)}

A

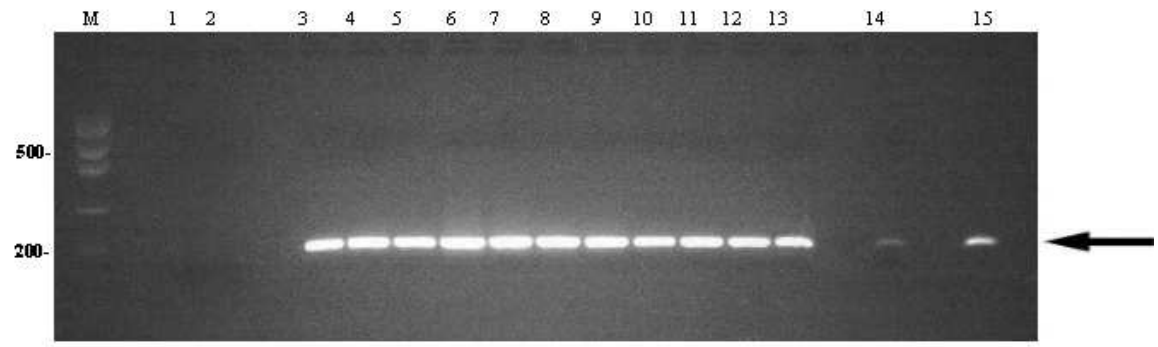
M 1 2 3 4 5 6 7 8 9 10 11 12 13 14 15
500-
200-

B

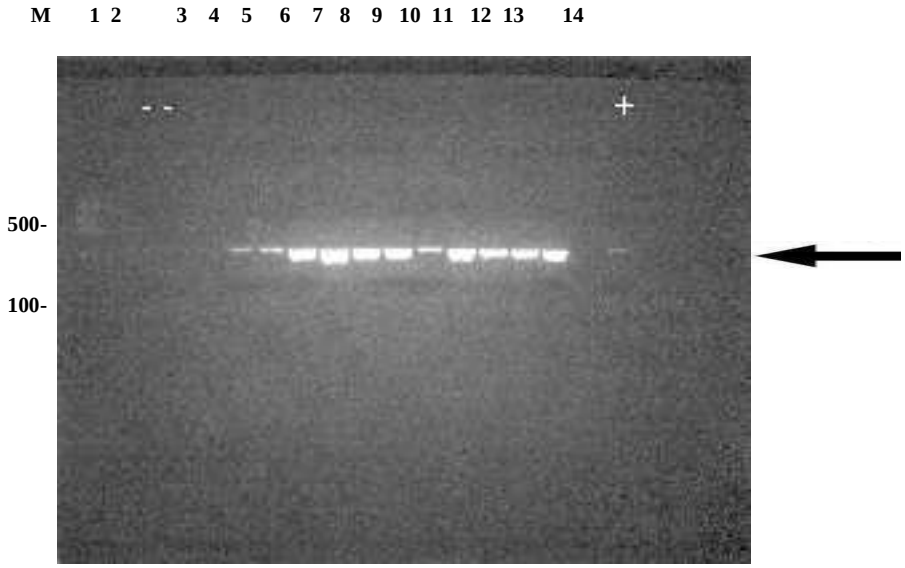
M 1 2 3 4 5 6 7 8 9 10 11 12 13 14
- -
+
500-
100-

C

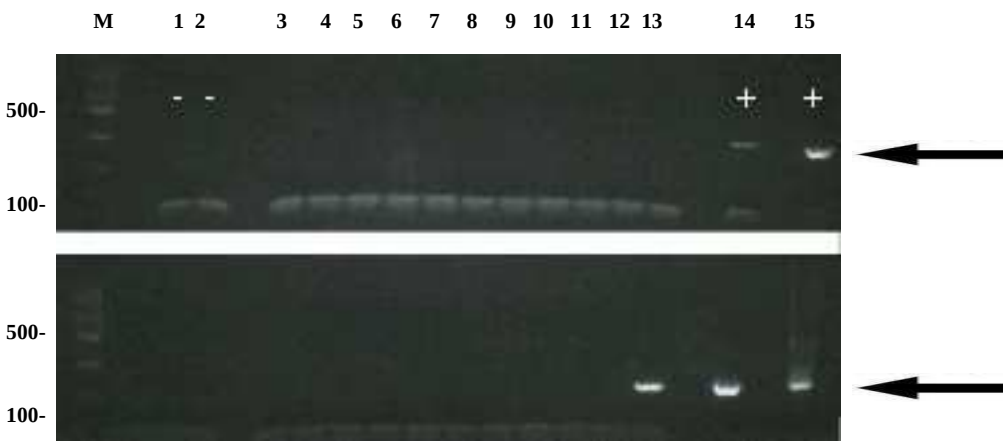
M 1 2 3 4 5 6 7 8 9 10 11 12 13 14 15
- -
+ +
500-
100-
500-
100-

Table 12: Results of the 16S rRNA, IS1245, and IS900 nested PCR Assays on Positive Bactec Subcultures

Sample Code	16 S rRNA PCR Result	IS1245 PCR Result	IS900 PCR Result	Conclusion
8	+	+	-	MAV
8E	+	+	-	MAV
11	+	+	-	MAV
11E	+	+	-	MAV
12	+	+	-	MAV
12E	+	+	-	MAV
13E	+	+	-	MAV
19E	+	+	-	MAV
21	+	+	-	MAV
21E	+	+	-	MAV
22	+	+	-	MAV
22E	+	+	-	MAV
24E	+	+	-	MAV
25	+	+	-	MAV
25E	+	+	-	MAV
32	+	+	-	MAV
41	+	+	-	MAV
47	+	+	-	MAV
62E	+	+	-	MAV
67	+	+	-	MAV
68	-	+	-	MAV
71	-	-	-	Other than MAC
71E	-	-	-	Other than MAC
83	+	+	-	MAV
92	+	+	-	MAV
92E	+	+	+	MAP

Mycobacterial Growth in MGIT Media

All MGIT culture tubes were evaluated for microbial activity based upon the fluorescence of the oxygen indicator and the level of turbidity. After six to eight weeks of incubation at 37°C with 5% CO_2, specimens suspected of mycobacterial growth were prepared for genomic DNA extraction and further PCR analysis analogous to the Bactec samples. The average time span from processing to harvesting was 8-10 weeks. Microscopic evaluation was performed on all MGIT samples that indicated the presence of bacterial respiration and growth which indicated the presence acid-fast positive bacteria. Samples that were acid-fast positive were then subjected to PCR investigation using primers specific for the 193 bp 16S rRNA sequence indicative of MAC and nested PCR for the 298 bp portion of the IS900 insertional element indicative of MAP. The results of the 16S rRNA assay showed 6/100 whereas, MAP was detected in 20/100 following nested PCR. Figure 14 illustrates the 16 S rRNA PCR results, whereas Figure 15 illustrates the nested PCR results for a representative set of positive isolates.

Figure 14. 16 S rRNA PCR Assay Results on a Representative Set of MGIT Cultures.

M corresponds to a 1 Kb 100 bp DNA step ladder. Lanes 1 & 2 correspond to negative controls. Lane 3=MS16, Lane 4=MS17, Lane 5=MS18, Lane 6=MS19, Lane 7=MS20, Lane 8=MS21, Lane 9=MS22, Lane 10=MS23, Lane 11=MS24, Lane 12=MS25, Lane 13=MS26, Lane 14=MS27, Lane 15=MS28, Lane 16=MS29, Lane 17=MS30. Lanes 18 & 19=positive controls (MAV; 193 bp & MAP; 193 bp, respectively).

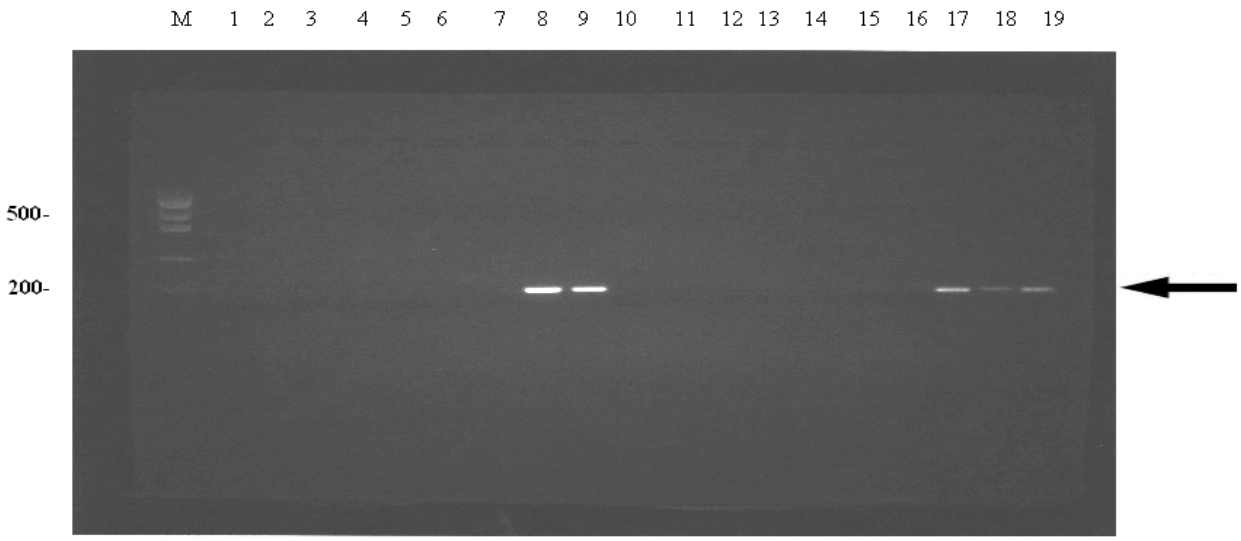
M 1 2 3 4 5 6 7 8 9 10 11 12 13 14 15 16 17 18 19
500-
200-

Figure 15. IS900 Nested PCR Assay Results for a Representative Set of MGIT Cultures.

(A) corresponds to a gel containing samples after the 1st round of amplification using P90/P91 primers. M corresponds to a 1 Kb 100 bp DNA step ladder. Lane 1=negative control, Lane 2=MS44, Lane 3=MS45, Lane 4=MS46, Lane 5=MS47, Lane 6=MS48, Lane 7=MS49, Lane 8=MS50, Lane 9=MS51, Lane 10=MS52, Lane 11=MS53, Lane 12=positive control (MAP; 401 bp), Lane 13=negative control, Lane 14=positive control (MAP; 401 bp). (B) corresponds to a gel containing samples after the 2nd round of amplification using Av1/Av2 primers. M1 corresponds to a 1 Kb 100 bp DNA step ladder. M2 corresponds to a 1 Kb 25 bp DNA step ladder. Lane 1=negative control, Lane 2=positive control (MAP; 298 bp), Lane 3=negative control, Lane 4=MS44, Lane 5=MS45, Lane 6=MS46, Lane 7=MS47, Lane 8=MS48, Lane 9=MS49, Lane 10=MS50, Lane 11=MS51, Lane 12=MS52, Lane 13=MS53, Lane 14=positive control (MAP; 298 bp), Lane 15=negative control.

A

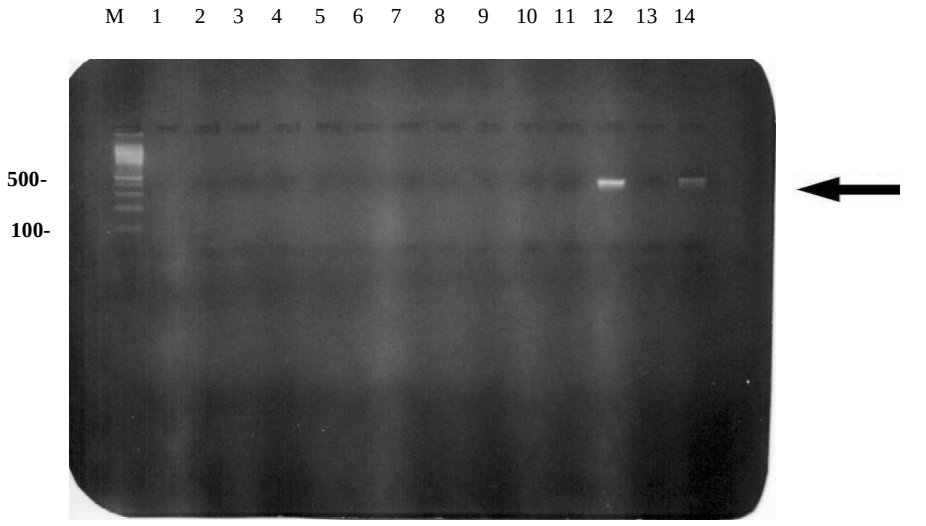
M 1 2 3 4 5 6 7 8 9 10 11 12 13 14
500-
100-

B

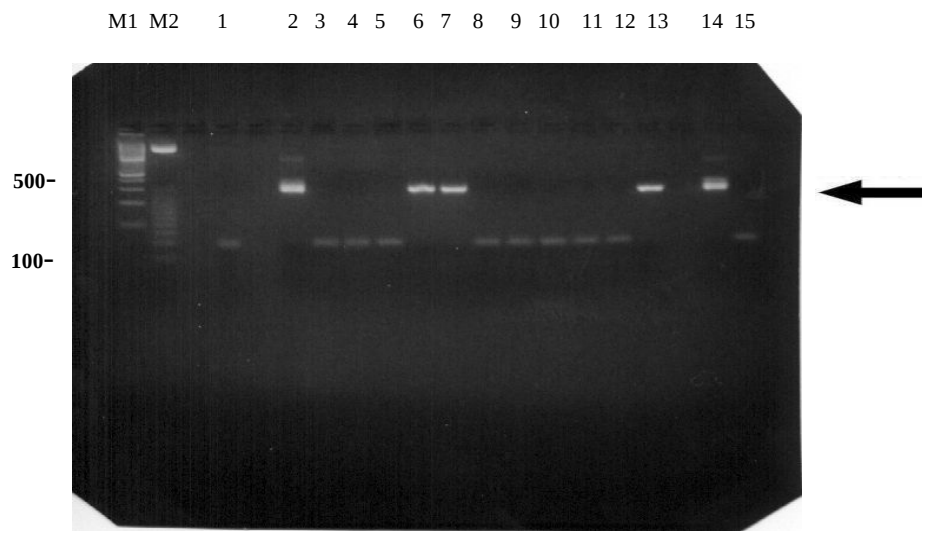
M1 M2 1 2 3 4 5 6 7 8 9 10 11 12 13 14 15
500-
100-

Sequence Analysis of Amplified IS900 DNA Fragments

The initial goal of DNA sequencing and analysis was to provide further support of positive PCR results by confirming the presence of the IS900 gene specific to MAP in mycobacterial isolates. The second objective of this exercise was to demonstrate homology to previously published MAP nucleotide sequences while investigating any variability among specific isolates obtained in this study. Seven samples that gave positive Av1/Av2 PCR results for the 298 bp IS900 fragment were selected as a representative set for DNA sequencing and subsequent analysis. Comparative computer analysis using Blast demonstrated that the seven nucleotide sequences obtained from CD tissues were homologs of the IS900 insertional sequence specific to MAP found in the GenBank database (Af416985). Figure 16 shows an alignment of the Blast results compared to a known bovine derived IS900 gene sequence. As shown in Table 13, 6/7 sample DNA sequences had a G+C content of approximately 60%, analogous to that of the mycobacterial genome (67%). The exception was sample MS70 which contained two mismatches where thymine was substituted for cytosine as well as an adenine and thymine insertion. Consequently, the G+C content of the MS70 nucleotide sequence was calculated to be 52%, much lower than the expected 67% that is usually observed in mycobacterial sequences. Sample sequences MS43 and MS47 were 100% homologous to the MAP IS900 gene, while sample sequence MS46 showed 99% identity with the standard IS900 gene. MS46 contained one mismatch in which a guanine was substituted for an adenine at the 218 bp position. Further analysis revealed that the MS53 nucleotide sequence also shared 99% homology with the IS900 element. Again, one mismatch was found in MS53 whereby the nucleotide adenine replaced an expected guanine at the 260 bp position. Sample MS73 was also 99% complementary to the

standard IS900 sequence containing one thymine insertion between base pairs 202 and 203. Sample MS92e again had 99% homology to the IS900 Map gene with an adenine insertion between base pair 226 and 227. Finally, sample sequence MS70 showed the most strain diversity having 96% identity with the standard IS900 MAP gene. MS70 contained two mismatches where thymine was substituted for cytosine at base pair positions 198 and 201. MS70 had an additional two nucleotide insertions in which an adenine was added between base pairs 161 and 162 and a thymine was inserted between base pairs 202 and 203. Further alignment and pairwise comparison analysis revealed that strain diversity among the seven IS900 amplified sequences was confined to the area between base pairs 148-260. Homology rates among the IS900 strains were similar to that observed when compared against bovine MAP. Nucleotides contained within base pairs 261-376 showed no variability compared to the IS900 gene.

Table 13: Pairwise Comparison Matrix of IS900 Nucleotide Sequences

Sample Code	GC Content	IS900 Identity	MS43 Identity	MS46 Identity	MS47 Identity	MS53 Identity	MS70 Identity	MS73 Identity	MS92e Identity
MS43	59.72%	100.00%	--	99.54%	100.00%	99.54%	98.15%	99.54%	99.54%
MS46	60.52%	99.58%	99.58%	--	99.58%	99.15%	97.86%	99.15%	99.15%
MS47	59.21%	100.00%	100.00%	99.57%	--	99.57%	98.25%	99.57%	99.57%
MS53	59.66%	99.58%	99.58%	99.15%	99.58%	--	98.29%	99.15%	99.15%
MS70	52.83%	94.94%	96.23%	95.29%	96.23%	96.23%	--	97.17%	95.29%
MS73	60.61%	99.58%	99.57%	99.14%	99.57%	99.14%	98.71%	--	94.14%
MS92e	59.03%	99.58%	99.56%	99.12%	99.56%	99.12%	97.80%	99.12%	--

Figure 16. Alignment of IS900 Blast Results following Nucleotide Sequencing.

```
TTGAGAGATGCGAT-TGGATCGCTGTGTGAAGGACACGTCGGCGTGGTCGTCTGCT-GGGTT      IS900* bp(148-207)
            ...................................................      MS43
..............................................................      MS46
..............................................................      MS47
..............................................................      MS53
  ............A.....................................T..T.T.....      MS70
  .............................................................T.      MS73
..............................................................      MS92e

GATCTGGACAATGACGGT-TACGGAGGTGGTTGTGGCACAACCTGTCTGGGCGGGCGTGGA      IS900* bp (208-267)
..........................................................          MS43
..........G...............................................          MS46
..........................................................          MS47
..........................................A...............          MS53
..........                                                          MS70
..........................................................          MS73
..........A...............................................          MS92e

CGCCGGTAAGGCCGACCATTACTGCATGGTTATTAACGACGACGCGCAGCGATTGCTCTC      IS900* bp (268-327)
............................................................        MS43
............................................................        MS46
............................................................        MS47
............................................................        MS53
                                                                    MS70
............................................................        MS73
............................................................        MS92e

GCAGCGGGTGGCCAACGACGAGGCCGCGCTGCTGGAGTTGATTGCGGCGG                 IS900* bp (328-376)
.........................................                           MS43
................................................                    MS46
.........................................                           MS47
................................................                    MS53
                                                                    MS70
................................................                    MS73
.........................................                           MS92e
```

IS900* = GenBank reference number AF416985, MAP 1453 bp; bovine source.

DISCUSSION

The specific role of mycobacteria in the pathogenesis of Inflammatory Bowel diseases, namely CD, remains controversial despite remarkable similarities to JD, known to be caused by MAP in ruminants. Current research points to a multi-factorial origin for CD involving genetic mutations in a key inflammatory pathway that allow for mycobacterial infection. This is followed by an abnormal, heightened immune response which only serves to perpetuate disease progression. The nature of MAP in its pathogenic form as a spheroplast coupled with inhibitors and inconsistencies in laboratory techniques complicates its detection. A clear understanding of CD etiology is further confounded by the co-existence of MAC subspecies, particularly MAV, in CD tissues obtained from the same patient. Co-infection of IBD patients may result from the interaction of several factors such as a compromised immune system. Cases of UC and CD co-infection have been recently reported in many IBD patients as well as in HIV patients. Another factor that might contribute to co-infection of MAC bacteria is the close evolutionary relationships among members of the MAC and their ability to share genetic information. Recently, the complete MAP genome sequence was published on the web site of the University of Minnesota (www.cbc.umn.edu/ResearchProjects/AGAC/Mptb/Mptbhome.html). The report showed that MAC bacteria have greater than 99% genomic homology, with only 22 genes, including the IS900 transposable element, that distinguish MAP from the remaining MAC members. These findings suggest that the etiological spectrum of IBD and CD is broadening

with regard to specific pathogens. Consequently, an effective, efficient protocol is urgently needed for the detection and identification of closely related MAC isolates that could facilitate a clearer picture of IBD and CD etiology, thereby enhancing diagnosis and treatment. The successful development and application of a molecular diagnostic typing protocol such as this is especially significant in those cases where simultaneous infection is common in order to differentiate between diseases present in the same patient. Therefore, the identification of a common PCR reaction mixture and a thermocycler protocol for the three PCR assays used in this study has considerably enhanced the level of accuracy, sensitivity, and time needed to identify pathogen(s) in clinical samples, most importantly, those mycobacterial agents involved in the etiology of IBD. It is noteworthy to mention that careful optimization reduced the time needed to run each PCR assay by half which may have great impact on future mycobacterial diagnosis. Furthermore, such assays will resolve the accurate identification of closely related isolates that commonly co-exist in the environment and co-infect vulnerable hosts as was observed in this study.

Data generated from our limited sequence analysis on seven isolates investigated in this study is significant because two of them demonstrated 100% identity to MAP from Bovine sources and may further the understanding of CD epidemiology with regard to mode and source of MAP transmission to humans. Additionally, these findings support the hypothesis that CD might be a zoonotic disease, thereby providing more credibility to those seeking better pasteurization procedures for retail milk and other diary products. As discussed earlier, MAP is known to be the causative agent to JD which affects not only cattle, but goats, sheep and many other types of

domestic animals. Because MAP infiltrates the mother's milk supply, infection in young calves is immediate. Likewise, young children with limited immunity and genetic susceptibility who drink insufficiently pasteurized milk are at risk for the development of IBD mainly CD. It is not the number of MAP isolates cultured from CD tissue that share homology to Bovine MAP that is significant but the fact that Bovine MAP may cause CD in humans. The other five MAP isolates that were investigated in this study have also shown significant homology to the IS900 gene derived from Bovine MAP. Because IS900 genes from other animal sources have yet to be sequenced, the specific identity and source of these isolates cannot be determined. However, the observed polymorphisms in these IS900 sequences may potentially match isolates from goats, sheep, or other animals and implicate the possibility of higher transmission risks to humans.

Sequence information gathered on members of MAC, namely MAP, from IBD patients may also have a far-reaching impact on determining the epidemiological versus geographical distribution of CD as it relates to high-risk regions for disease transmission. Collection of molecular information into a national or world-wide database would provide documentation of such areas and may contribute to improved specificity of diagnosis and treatment of CD at the molecular level.

CONCLUSION

In summary, 1) the PCR panel developed in this study provides a specific and rapid tool for the identification of members of the MAC in clinical samples and culture via molecular typing. 2) Members of the MAC including MAP have been isolated from IBD patients suggesting a mycobacterial role regarding this chronic and controversial disease. 3) The sequence analysis of seven IS900 amplicons supports CD as an environmental health risk in regard to products derived from domesticated animals, and 4) the genetic diversity of the isolates investigated here emphasizes the need for a database that can document all MAC isolates from IBD patients for a better understanding of geographical CD hot spots versus epidemiology. The impact of these findings is significant toward etiology, rapid diagnosis, improved treatments, and better prevention and control of CD.

Ultimately, this pilot study suggests that a larger scale investigation with regard to the presence of MAP in clinical samples from IBD patients is urgently needed. I am pleased to report that since the conclusion of performing these experiments, an expanded study has been approved and funded by the National Institute of Health (USA) to be carried out in Dr. Naser's laboratory at the University of Central Florida. This signifies the importance of the preliminary data reported in this study.

LIST OF REFERENCES

1. **Bannantine JP, Qing Zhang, Ling-Ling Li, and Vivek Kapur**. 2003. Genomic homogeneity between Mycobacterium avium subsp. avium and Mycobacterium avium subsp. paratuberculosis belies their divergent growth rates. BMC Microbiol. 3(1):10.

2. **Bayless TM, Tokayer AZ, Polito JM 2nd, Quaskey SA, Mellits ED, Harris ML**. 1996. Crohn's disease: concordance for site and clinical type in affected family members--potential hereditary influences. Gastroenterology. 111(3):573-9.

3. **Berrebi D, Maudinas R, Hugot JP, Chamaillard M, Chareyre F, De Lagausie P**. 2003. CARD 15 gene overexpression in mononuclear and epithelial cells of the inflamed Crohn's disease colon. Gut. 52(6):840-6.

4. **Bouma G and Strober W**. 2003. The Immunological and genetic basis of inflammatory bowel disease. Nature Reviews Immunology. 3(7):521-533.

5. **Bull Tj, McMinn EJ, Sidi-Boumedine K, Skull A, Durkin D, Neild P, Rhodes G,**. 2003. Detection and Verification of Mycobacterium avium subsp. paratuberculosis in Fresh Ileocolonic Mucosal Biopsy Specimens from Individuals with and without Crohn's Disease. Journal of Clinical Microbiology. 41(7):2915-2923.

6. **Bull TJ, McMinn EJ, Sidi-Boumedine K, Skull A, Durkin D, Neild P, Rhodes G, Pickup R, Hermon-Taylor J**. 2003. Detection and verification of Mycobacterium avium subsp.

paratuberculosis in fresh ileocolonic mucosal biopsy specimens from individuals with and without Crohn's disease. J Clin Microbiol. 41:2915-2923.

7. **Chamaillard M, Girardin SE, Viala J, and Philpott DJ**. 2003. Nods, Nalps, and Naip: intracellular regulators of bacterial-induced inflammation. Cell Microbiol. 5(9):581-92.

8. **Chamberlin W, Graham DY, Hulten K, El-Zimaity HM Schwartz MR, Naser S, Shaf**. 2001. Review article: Mycobacterium avium subsp. Paratuberculosis as one cause of Crohn's disease. Ailment Parmacol Ther. 15(3):337-46.

9. **Chamberlin, W., Graham, D.Y., Hulten, K., El-Zimaity, H.M., Schwartz, M.R., Naser, S., Shafran, I., and El-Zaatari, F.A.K**. 2001. Review article: Mycobacterium avium subsp. Paratuberculosis as one cause of Crohn's disease. Ailement Pharmacol Ther. 15:337-346.

10. **Chiodini RJ**. 1989. Crohn's Disease and the Mycobacterioses: a Review and Comparison of Two Disease Entities. Clin Microbiol Rev. 2:90-117.

11. **Chiodini RJ, Kruiningen HJ, Thayer WR, Coutu JA**. 1984. Characteristics of an unclassified Mycobacterium species isolated from patients with Crohn's disease. J Clin Microbiol. 20:966-971.

12. **Chiodini RJ, Van Kruiningen HJ, Thayer WR, Merkal RS, and Coutu JA**. 1984. Possible role of mycobacteria in inflammatory bowel disease. I. An unclassified Mycobacterium species isolated from patients with Crohn's disease. Dig Dis Sci. 29(12):1073-9.

13. **Cocito C, Gilot P, Coene M, de Kesel M, Poupart P, and Vannuffel P**. 1994. Paratuberculosis. Clin Microbiol Rev. 7: 328-345.

14. **Crohn BB, Ginzburg K, and Oppenheimer GD**. 1932. Regional Illeitis: a Pathological and Clinical Entity. J. Am. Med. Assoc. 99:1323-1329.

15. Crohn's Disease and Colitis Foundation Report on Crohn's Disease.

http://www.ccfa.org/medcentral

16. **Cuthbert AP, Fisher SA, Mirza MM, King K, Hampe J, Croucher PJ, Mascheretti S, Sanderson J, Forbes A, Mansfield J, Schreiber S, Lewis CM, Mathew CG** . 2002. The contribution of NOD2 gene mutations to the risk and site of disease in inflammatory bowel disease. Gastroenterology. 122(4):867-74.

17. **Dalziel TK**. 1913. Chronic Interstitial Enteritis. Br. Med J.. ii:1068-1070.

18. **Ebert EC, Bhatt BD, Liu S, and Das KM**. 1991. Induction of Suppressor Cells by Mycobacterium paratuberculosis Antigen in Inflammatory Bowel Disease. Clin Exp Immunol. 83(2):320-325.

19. **El-Zaatari FAK, Naser SA, Engstrand L, Burch PE, Hachem CY, Whipple DL, and Graham DY**. 1995. Nucleotide Sequence Analysis and Seroreactivities of the 65K Heat Shock Protein from Mycobacterium paratuberculosis. Clin Diag Lab Immunol. 2(6):657-664.

20. **El-Zaatari FAK, Osato MS and Graham DY**. 2001. Etiology of Crohn's Disease: the role of Mycobacterium avium paratuberculosis. Trends in Molecular Medicine. 7(6):247-52.

21. **Ellingson JLE, Stabel JR, Bishai WR, Frothingham R, and Miller JM**. 2000. Evaluation of the accuracy and reproducibility of a practical PCR panel assay for rapid detection and differentiation of Mycobacterium avium subspecies. Molecular and Cellular Probes. 14:153-161.

22. Possible links between Crohn's disease and Paratuberculosis.

http://europa.eu.int/comm/food/fs/sc/scah/out38_en.pdf

23. **Gibson PR**. 1990. Current concepts in pathogensis of Crohn's disease. J Gastroenterol Hepatol. 5:44-65.

24. **Gilles Etienne, Christelle Villenueve, Helen Billman-Jacobe, Catherine Asta**. 2002. The impact of the absence of glycopeptidolipids on the ultrastructure, cell surface and cell wall properties, and phagocytosis of Mycobacterium smegmatis. Microbiology. 148:3089-3100.

25. **Grant IR, Ball HR, Rowe MT**. 1993. Isolation of Mycobacterium paratuberculosis from milk by immunomagnetic separation. Appl Environ Microbiol. 64:3156-8.

26. **Greenstein RJ**. 2003. Is Crohn's disease caused by a mycobacterium? Comparisons with leprosy, tuberculosis and Johne's disease. Lancet Infect Dis. 3(8):507-14.

27. **Gui GP, Thomas PR, Tizard MI, Lake J, Sanderson JD, Hermon-Taylor J**. 1997. Two-year-outcomes analysis of Crohn's disease treated with rifabutin and macrolide antibiotics. J Antimicrob Chemother. 39(3): 393-400.

28. **Hazra R, Lee SH, Maslow JN, Husson RN**. 2002. Related strains of Mycobacterium avium cause disease in children with AIDS. J Infect Dis. 181(4):1298-303.

29. **Hermon-Taylor J, Bull TJ, Sheridan JM, Cheng J, Stellakis ML, Sumar N**. 2000. Causation of Crohn's disease by Mycobacterium avium subspecies paratuberculosis. Can J Gastroenerol. 14(6):521-39.

30. **Homuth M, Valentin-Weigand P, Rohode M, and Gerlach GF**. 1998. Identification and Characterization of a Novel Extracellular Reductase from Mycobacterium paratuberculosis. Infection and Immunology. 66(2):710-16.

31. **Hugot JP, Zoulai H, and Lesage S**. 2003. Lessons to be learned from the NOD2 gene in Crohn's disease. Eur J Gastroenterol Hepatol. 15(6):593-7.

32. **Hulten K, El-Zimaity HM, Karttunen TJ Alashhrawi A, Schwartz MR, Graham DY, and El Zaatari FAK**. 2001. Detection of Mycobacterium avium subspecies paratuberculosis in Crohn's diseased tissues by in situ hybridization. Am J Gastroenerol. 96:1529-1535.

33. **Hulten K, Karttunen TJ, El-Zimaity HM, Naser SA, Almashhrawi A, Graham DY, and El-Zaatari FAK**. 2000. In situ method for studies of cell wall deficient M. paratuberculosis in tissue samples. Vet Microbiol. 77(3-4):513-8.

34. **Inohara N, Ogura Y, and Nunez G**. 2002. Nods: a family of cytosolic proteins that regulate the host response to pathogens. Curr Opin Microbiol. 5(1):76-80.

35. Anti-mycobacterial treatment and Crohn's Disease.

http://alan.kennedy.name/crohns/chemo.htm

36. **Kirsner J**. 1984. Landmark Perspective: Crohn's Disease. JAMA. 251:80-81.

37. **Kugathasan S, Judd RH, Hoffmann RG, Heikenen J, Telega G, Khan F, Weisdorf-Schindele S, San Pablo W Jr, Perrault J, Park R, Yaffe M, Brown C, Rivera-Bennett MT, Halabi I, Martinez A, Blank E, Werin SL, Rudolph CD, Binion DG**. 2003. Epidemiologic and clinical characteristics of children with newly diagnosed inflammatory bowel disease in Wisconsin: a statewide population-based study. Journal of Pediatrics. 143(4):525-31.

38. Paratuberculosis - Johne's Disease - History.

http://www.husdyr.kvl.dk/htm/ssn/history.htm

39. **Lakatos L**. 2000. Immunology of Inflammatory Bowel disease. Acta Physiol Hung. 87(4): 355-372.

40. **Lala S, Ogura Y, Osborne C, Hor SY, Bromfield A, Davies S, Ogunbiyi O, Nunez G, and Keshav S**. 2003. Crohn's disease and the NOD2 gene: a role for paneth cells. Gastroenterology. 125(1):47-57.

41. **Lemassu A and Daffe M**. 1994. Structural features of the extracellular polysaccharides of Mycobacterium tuberculosis. Biochemistry Journal. 297(pt2):351-7.

42. **Leonardo AS, Mura M, Tanda F, Lissia A, Solinas A, Fadda G, and Zanetti S**. 2001. Identification of Mycobacterium avium subsp. Paratuberculosis in Biopsy Specimens from Patients with Crohn's Disease Identified by In Situ Hybridization. Journal of Clinical Microbiology. 4514-4517.

43. **Loftus EV Jr, Schoenfeld P, Sandborn WJ**. 2002. The epidemiology and natural history of Crohn's Disease in population-based patient cohorts from North America: a systematic review. Ailment Pharmacol Ther. 16(1): 51-60.

44. **Loftus Jr EV, Silverstein MD, Sandborn WJ, Tremaine WJ, Harmsen WS, and Zinsmeister AR**. 1998. Crohn's Disease in Olmsted County, Minnesota, 1940-1993: Incidence, Prevalence, and Survival. Gastroenterology. 114:1161-1168.

45. **Madigan MT, Martinko JM, and Parker J**: Brock Bilogy of Microorganisms, NJ: Prentice Hall, 2003.

46. **Markesich DC, El-Zaatari FAK, Graham DY**. 1993. Activitiy of clarithromycin against intracellular Mycobacterium paratuberculosis-Putative agent of Crohns' disease. Eur J Gastroenterol Hepatol. 5:613-15.

47. **Markesich DC, Graham DY and Yoshimura HH**. 1988. Progress in Culture and Subculture of Spheroplasts and Fastidious Acid-Fast Bacilli Isolated from Intestinal Tissues. J Clin Microbiol. 26(8):1600-1603.

48. **Millar D, Ford J, Sanderson J, Withey S, Tizard M, Doran T, Hermon-Taylor J**. 1996. IS900 PCR to detect Mycobacterium paratuberculosis in retail supplies of whole pasteurized cow's milk in England and Wales. Appl Environ Microbiol. 62:3446-52.

49. **Mishna D, Katsel P, Brown ST, Gilberts ECAM, and Greenstein RJ**. 1996. On the etiology of Crohn's disease. Proc Natl Acad Sci. 93:9816-9820.

50. **Modigliani R, Mary JY, Simon JF, Cortot A, Soule JC, and Gendre JP**. 1990. Clinical, Biological and Endoscopic Picture of Attacks of Crohn's Disease. Gastroenterology. 98:811-818.

51. **Momotani E, Whipple DL, Thiermann AB and Cheville NF**. 1998. Role of M cells and macrophages in the entrance of Mycobacterium paratuberculosis into domes of ileal Peyer's patches in calves. Vet. Pathol.. 25(2):131-7.

52. **Moschowitz E and Wilensky A**. 1923. Nonspecific granulomata of the intestine. Am J Med Sci. 166:48-66.

53. **Naser SA, Felix J, Liping H, Romero C, Naser N, Walsh A, Safranek W**. 1999. Occurrence of the IS900 gene in Mycobacterium avium complex derived from HIV patients. Mol Cell Probes. 13(5):367-72.

54. **Naser SA, Shafran I, Schwartz D, El-Zaatari, and Biggerstaff J**. 2002. In situ Identification of mycobacteria in Crohn's disease patient tissue using confocal scanning laser microscopy. Molecular and Cellular Probes. 16:41-48.

55. **Naser SA, Shwartz D, and Shafran I**. 2000. Isolation of Mycobacterium avium subsp paratuberculosis From Breast Milk of. Am J Gastroenterol. 95(4): 1094-5.

56. NCBI website. **http://www.ncbi.nlm.nih.gov/**

57. NIH Report on Crohn's Disease. 1998 . NIH Publication No. 98-3410.

http://www.niddk.nih.gov/health/digest/

58. **Ogura Y, Bonen DK, Inohara N, Nicolae DL, Chen FF, Ramos R, Britton H, Mora**. 2001. A frameshift mutation in NOD2 associated with susceptibility to Crohn's disease. Nature. 411(6837):603-6.

59. Annual report of Innate immunity and cell signaling for year 2002.

http://www.pasteur.fr/recherche/RAR/RAR2002/Imis-en.html

60. Mycobacteriology. **http://www2.provlab.ab.ca/bugs/mycob/mycobact.htm**

61. **Rosenstiel P, Fantini M, Brautigam K, Kuhbacher T,Waetzig GH, Seegert D, and Schreiber S**. 2003. TNF-alpha and INF-gamma regulate the expression of the NOD2 (CARD15) gene in human intestinal epithelial cells. Gastroenterology. 124(4):1145-9.

62. **Satsangi J, Jewell DP, Bell JI**. 1997. Genetics of Crohn's Disease. Gut. 40(5):572-4.

63. **Satsangi J, Jewell DP, Rosenberg WMC, Bell JI**. 1994. Genetics of Inflammatory Bowel Disease: A progress Report. Gut. 35:696-700.

64. **Schwartz D, Shafran I, Romero C, Piromalli C, Biggerstaff J, Naser N, Chamberlin W, Naser SA** . 2000. Use of shrt-term culture for identification of Mycobacterium avium subsp. p. Clin Microbiol Infect. 6:303-307.

65. **Shanahan Fergus**. 2002. Crohn's Disease. Lancet. 359:62-69.

66. **Sheridan JM, Bull TJ, Hermon-Taylor J**. 2003. Use of bioinfomatics to predict a function for the GS element in Mycobacter. Journal of Mol Microbiol Biotechnology. 5(1):57-66.

67. **Shivananda S, Lennard-Jones JE, Logan RF, Fear N, Price A, Carpenter L, Van**. 1996. Incidence of Inflammatory bowel disease across Europe: Is there a difference between north and south? Results of the European collaborative study on inflammatory bowel disease (EC-BID). Gut. 39:690-7.

68. St. George's Hospital Medical School Website.

http://www.sghms.ac.uk/Departments/crohns_DRG.htm

69. **Stabel JR**. 2001. On-farm batch pasteurization destroys Mycobacterium paratuberculosis in waste milk. Journal of Dairy Science. 84(2):524-7.

70. **Stahl DA and Urbance JW**. 1990. The division between fast- and slow-growing species correspondes to natural relationships among the mycobacteria. Journal of Bacteriology. 172(1): 166-24.

71. **Tan Trao V, Huong PL, Thuan AT, Long HT, Trach DD, Wright EP**. 1988. Responses to Mycobacterium leprae by lympocytes from new and old leprosy patients: role of exogenous lymphokines. Ann Institute Pasteur Immunol. 139(2):124-33.

72. **Tessema MZ, Koets AP, Rutten VP, Gruys E**. 2001. How does Mycobacterium avium subsp. Paratuberculosis resist intracellular degradation. Vet Q. 23(4):153-62.

73. Johne's Information Center. **http://www.johnes.org/history**

74. Crohn's Resource Homepage. **http://www.crohnsresource.com**

75. **Walmsley RS, Ibbotson JP, Chahal H, Allan RN**. 1996. Antibodies against Mycobacterium paratuberculosis in Crohn's disease. QJM. 89(3):217-21.

76. PCR Seminar. **http://www.biotechlab.nwu.edu/pe**

77. **Whittington RJ, Reddacliff L, Marsh I and V Saunders**. 1999. Detection of Mycobacterium avium subsp paratuberculosis in formalin-fixed paraffin-embedded intestinal tissue by IS900 polymerase chain reaction. Aust Vet J. 77(6):392-7.

78. **Yamamoto Y and Gaynor RB**. 2001. Theraputic potential of the NF-kB in the treatment of inflammation and cancer. J Clin Invest. 107(2):135-142.